energies

MDPI

Review

Inductive Power Transfer for Electric Vehicle Charging Applications: A Comprehensive Review

Emrullah Aydin [1,*], Mehmet Timur Aydemir [2], Ahmet Aksoz [3], Mohamed El Baghdadi [4] and Omar Hegazy [4]

[1] Department of Electrical and Electronics Engineering, Malatya Turgut Ozal University, 44210 Malatya, Turkey
[2] Department of Electrical and Electronics Engineering, Kadir Has University, 34083 Istanbul, Turkey; timur.aydemir@khas.edu.tr
[3] Department of Energy Science and Technology, Sivas Cumhuriyet University, 58140 Sivas, Turkey; aaksoz@cumhuriyet.edu.tr
[4] MOBI-EPOWERS Research Group, Department of Electrical Engineering and Energy Technology (ETEC), Vrije Universiteit Brussel (VUB), 1050 Brussels, Belgium; mohamed.el.baghdadi@vub.be (M.E.B.); omar.hegazy@vub.be (O.H.)
* Correspondence: emrullah.aydin@ozal.edu.tr; Tel.: +90-537-727-00-00

Abstract: Nowadays, Wireless Power Transfer (WPT) technology is receiving more attention in the automotive sector, introducing a safe, flexible and promising alternative to the standard battery chargers. Considering these advantages, charging electric vehicle (EV) batteries using the WPT method can be an important alternative to plug-in charging systems. This paper focuses on the Inductive Power Transfer (IPT) method, which is based on the magnetic coupling of coils exchanging power from a stationary primary unit to a secondary system onboard the EV. A comprehensive review has been performed on the history of the evolution, working principles and phenomena, design considerations, control methods and health issues of IPT systems, especially those based on EV charging. In particular, the coil design, operating frequency selection, efficiency values and the preferred compensation topologies in the literature have been discussed. The published guidelines and reports that have studied the effects of WPT systems on human health are also given. In addition, suggested methods in the literature for protection from exposure are discussed. The control section gives the common charging control techniques and focuses on the constant current-constant voltage (CC-CV) approach, which is usually used for EV battery chargers.

Keywords: wireless power transfer (WPT); Inductive Power Transfer; electric vehicles (EVs)

Citation: Aydin, E.; Aydemir, M.T.; Aksoz, A.; El Baghdadi, M.; Hegazy, O. Inductive Power Transfer for Electric Vehicle Charging Applications: A Comprehensive Review. *Energies* **2022**, *15*, 4962. https://doi.org/10.3390/en15144962

Academic Editor: Byoung Kuk Lee

Received: 20 May 2022
Accepted: 13 June 2022
Published: 6 July 2022

1. Introduction

The decrease in fossil fuel resources and the environmental pollution caused by their use has made it necessary to look towards renewable energy resources. Solar power plants, wind turbines, hydrogen energy, and wave energy are just a few of the methods used to generate electricity. Electricity can be produced by more than one method, and with sustainable production, interest in electric vehicles is increasing rapidly. Although the prices of electric vehicles are high at the time of first purchase, they have important advantages such as low maintenance costs compared to conventional vehicles with internal combustion engines and being able to travel at much lower prices per kilometer. In recent years, almost all the big vehicle manufacturers have announced that they will reduce the production of diesel- and gasoline-based vehicles and focus on hybrid and fully electric vehicles. However, before these vehicles are produced and put on the market, it is a necessity to establish battery charging stations and to realize alternative charging methods. Wireless charging is one of these methods for electric vehicle batteries. With this method, it is possible to easily charge the vehicles without the need for any cable connection to the vehicle and to increase the range by charging them in parking areas, while waiting at the

red traffic lights or when the vehicle is stopped at the garage. WPT systems due to the absence of physical contact or wired connections bring advantages such as ease of use, high safety, high reliability, low maintenance cost and long service life. Due to these advantages, it has a wide range of use not only with electric vehicles but also in applications such as mobile phones, biomedical implants, industries such as the space industry or textile and military applications [1–6].

There are three main wireless charging methods for EVs, and they are given in Figure 1. These are static, quasi-dynamic and dynamic charging. Static charging is the wireless charging of EVs in parking areas when it is in a stationary position. There are some limitations to this type of charging, such as limited overall driving range, typically long charging times, etc. Quasi-dynamic charging offers increased driving range along the trip, with charging pads implemented at the bus stations and at traffic light stops [7]. This means the EV can be charged not only during parking but also at temporary stops or while moving slowly. In dynamic charging, the primary track is buried into the road and spread, with the target to energize the EV during the trip while driving. The cost of dynamic charging is more than the other charging methods, but the most important problem of all EVs is the limited range, which can be eliminated with this method. A good review on cost comparisons for charging methods was performed by investigating two commercial product costs, and it seems that stationary charging is the most cost-effective method [8]. The main focus of this paper is a review of the stationary charging of EVs.

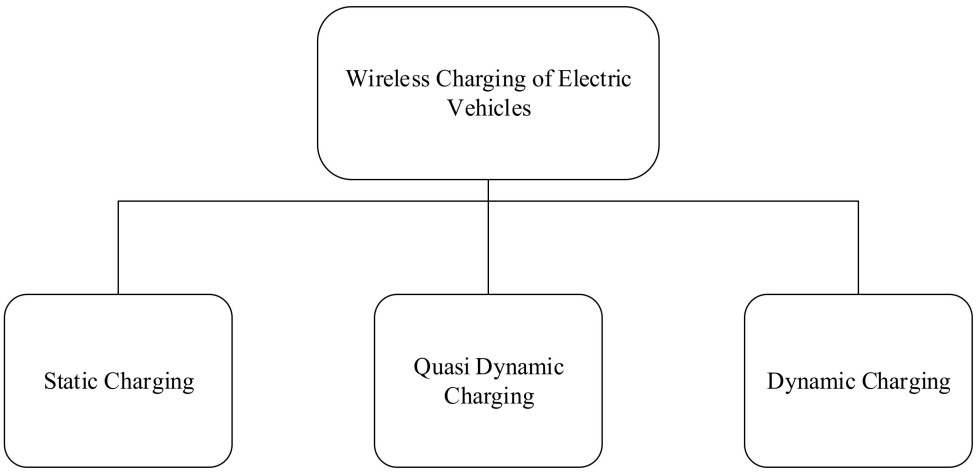

Figure 1. Wireless charging methods for EVs.

In this article, the parameters that are critical in the design of WPT systems, how and why they are selected in the studies in the literature and which methods are used more frequently are explained and shown with graphics. In addition, health standards and the compatibility of the proposed structures with these standards are emphasized. It is a study that design engineers can benefit from, especially when determining the parameters of a WPT system to be used in electric vehicle charging. This paper reviews IPT systems and is organized as follows. Section 1 presents the usage areas of WPT systems and why it is needed. In addition, a brief overview of types of Wireless charging methods for EV batteries is given. Section 2 explains the history of the evolution of WPT systems from the first time the idea was introduced up to the present. Section 3 describes the working principle of IPT systems and the fundamentals of this technology. In Section 4, comprehensive design considerations in IPT systems are given based on the related literature on the recent developments for design parameters, control methods and health issues. Most cited articles in the literature are given in tabular form in the Appendix A in Table A1.

2. History of WPT

In order to prove the mathematical theory put forward by James Clerk Maxwell in 1873, Heinrich Rudolf Hertz conducted a series of experiments in 1887, and as a result of these experiments, the existence of radio waves was revealed [9]. With the contribution of these developments, the idea of WPT was first put forward by Nikola Tesla in 1891. Tesla has conducted research towards the goal of transmitting electrical energy wirelessly around the world. For this purpose, in 1899, the construction of the Wardenclyffe Tower near Long Island Sound was started. The tower was never operational since the resources of the project were exhausted [10]. In order to see the development of WPT technology from past to present, the historical development is shown in Figure 2.

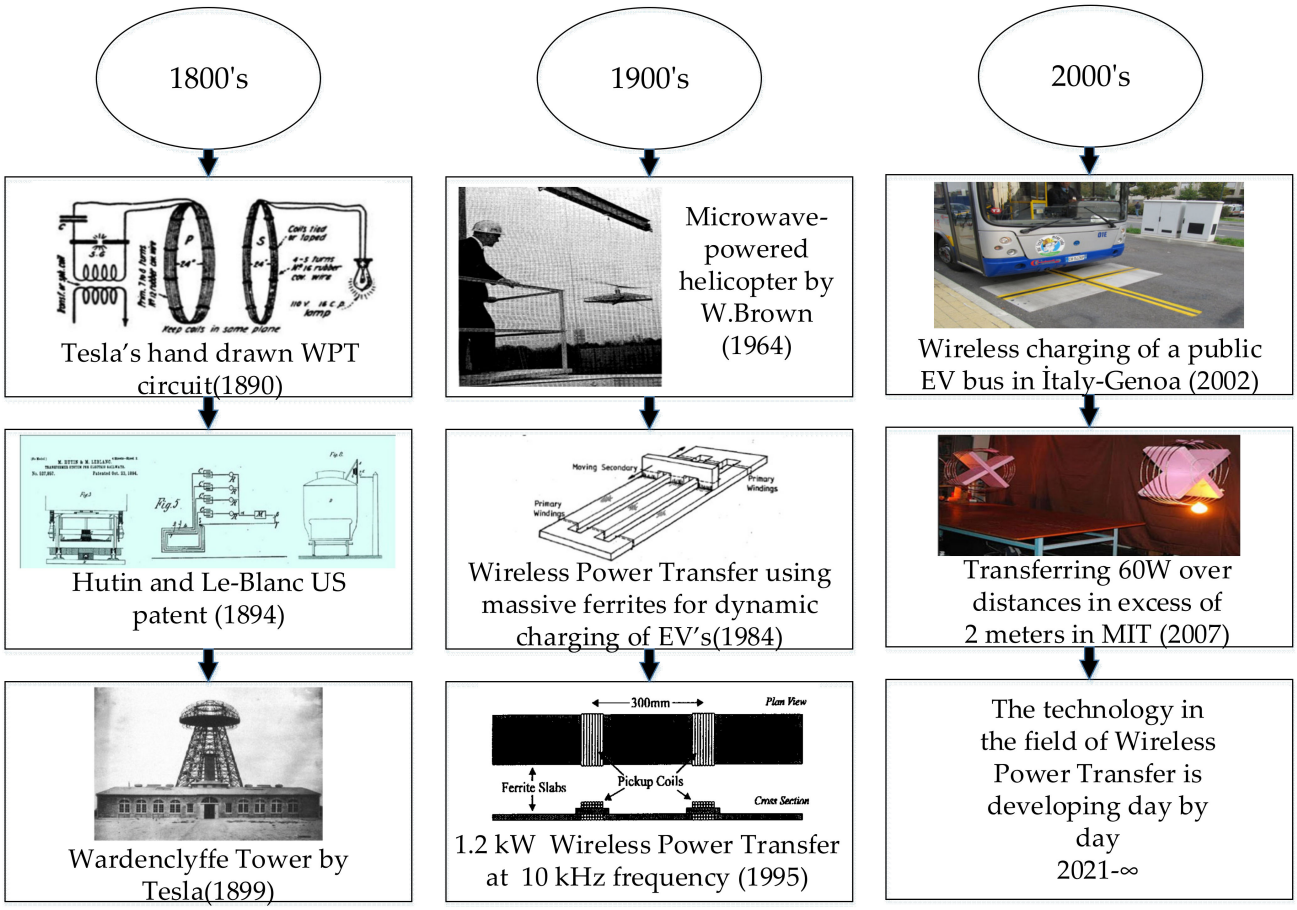

Figure 2. History of evolution of WPT [10–18].

In the late 1800s, only a few studies had been conducted aside from Tesla's discoveries. One of these studies was a patent registered by Hutin and Le-Blanc in 1894 [11], which was the first known idea for energizing Electric Vehicles wirelessly. With the end of the war period in the world, studies began to be published at the end of the 1900s. In 1964, with the invention of rectenna and the developments in microwave technology, William Brown tested the first microwave-powered helicopter [12]. The studies carried out in these examples were applications where power transfer was carried out from only a few millimeters of distance using a large amount of cores. In a study conducted in this period, it was aimed to transfer power from a distance of only a few millimeters between primary and secondary windings using a long ferrite bar [13]. In a study conducted in 1989, it was aimed to reduce the switching losses by connecting parallel capacitors to thyristors and to transfer high-efficiency wireless power. The power value of 500 W has been transferred as approximately 260 W with an efficiency of 52% [14]. The article author completed his doctoral thesis on this subject at Paris University in 1988, and this thesis is one of the

first doctoral dissertations in this field. There are similar works in the literature [15,16]. The dynamic wireless charging of an electric vehicle from a distance of 75 mm and at an alignment of ±400 mm and a power transfer of 1.2 kW was performed [17]. In the early 2000s, the idea of wirelessly charging electric vehicles was brought up in New Zealand. However, one of the first applications of this idea was carried out in 2002 in Genoa, Italy, in the electric bus project that charged busses wirelessly at the bus stop, as shown in Figure 2. The most important milestone after the idea of WPT was put forward by Tesla undoubtedly occurred in 2007, when a group of researchers at MIT powered a 60 W light bulb at a distance of more than 2 m [18]. Thus, the interest of scientists and technology companies around the world has increased, and the number studies on this subject has increased rapidly. Nowadays, by increasing the efficiency of WPT systems using newly proposed topologies and designs, the usage area of this technology is widening. In addition to these developments, there are still challenges to the wireless charging of EVs. Especially for long-distance travel, dynamic WPT systems can be preferred since the charging time is still the most important problem for EVs. However, this option is not cost effective. In addition, high-power EV charging has a significant effect on the grid system, which is another critical problem for the EVs and their charging methods. Moreover, by increasing the power and operating frequency, the magnetic field exposure becomes more important.

3. Fundamentals of IPT Systems

In this section, different types of WPT systems, basic features and working principles are explained. WPT systems can be grouped under three main headings in which power transfer can take place by magnetic coupling, capacitive coupling and microwave propagation. Microwaves are applications where power transfer occurs with low efficiency by using high frequencies over long distances. For short-distance power transfer, Inductive and Capacitive Power Transfer (CPT) systems are the most popular used systems. Capacitive Power Transfer has some limitations on the power levels and the transfer distance since it is based on a confined electric field distribution between two conductive plates [19,20]. Inductive Power Transfer (IPT) systems are the most frequently used and well-known power transmission systems that take advantage of magnetic flux distribution, applicable to all ranges of power and have considerably longer transfer distances than CPT systems. IPT systems are divided into two main groups according to the short and long distance between the coils. Due to the large distance between the coils in loosely coupled systems, the amount of leakage flux is high, and this is why it is named as such. Especially electric vehicle charging applications are considered in this group. In tightly coupled systems, there is a small gap between the coils, and the leakage fluxes are reduced and coupling is increased by using the core. The scheme of the basic classification of WPT systems is given in Figure 3.

In this work, loosely coupled IPT systems are reviewed. The operation of IPT systems is based on the same principles as those of transformers. In the conventional transformers, there is a ferrite core and the primary and secondary coils are wound around this core. However, WPT systems can have a large air-gap air core transformer with an appropriate capacitive compensation topology. The system basically consists of two coils which are magnetically coupled. Figure 4 shows a magnetically coupled IPT system.

In Figure 4, L_1 and L_2 are the primary and the secondary coils, and C_1 and C_2 are the compensation capacitors. M shows the mutual inductance, and ϕ_{l1} and ϕ_{l2} are the leakage flux for the primary and secondary sides, respectively. The coupling coefficient (k) equation is given below:

$$k = \frac{M}{\sqrt{L_1 L_2}} \tag{1}$$

Since the coupling coefficient value varies typically from 0.1 to 0.3 for a loosely coupled IPT system [21] for common low power EV charging applications, by adding compensation capacitors to work at resonance, a system that is highly efficient and more tolerant to

misalignment between the receiving coil can be obtained. The resonant frequency equation for a series RLC circuit is as follows:

$$\omega_0 = \frac{1}{\sqrt{LC}} \quad (2)$$

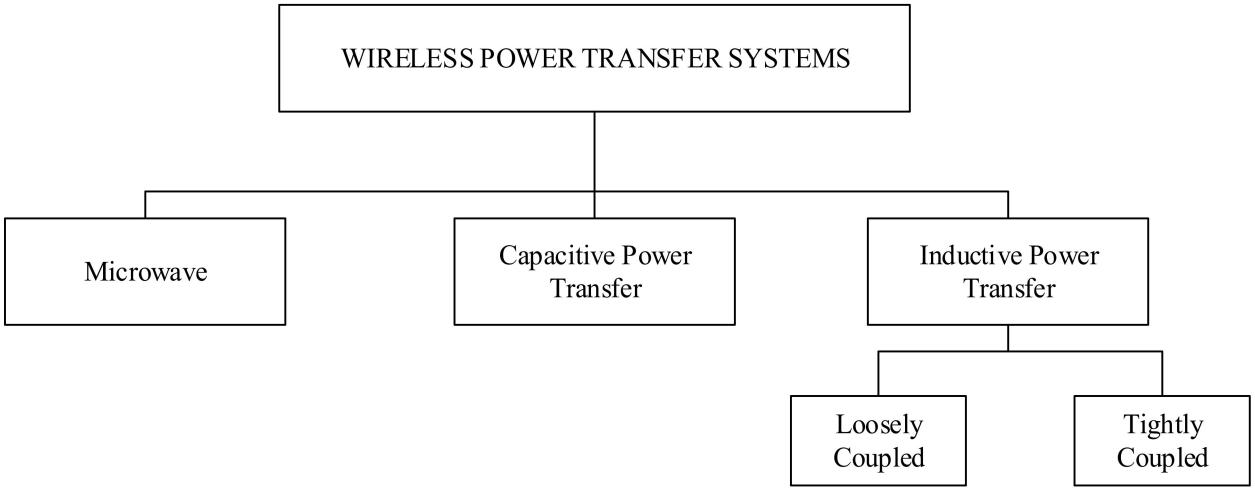

Figure 3. Classification of WPT.

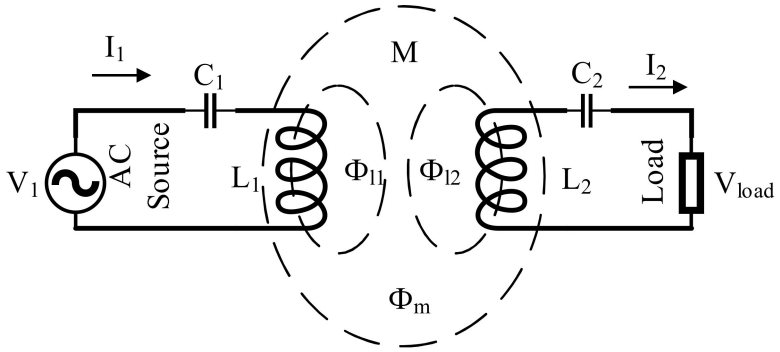

Figure 4. Fundamental structure of an IPT system.

The block diagram showing all components of an IPT system is given in Figure 5.

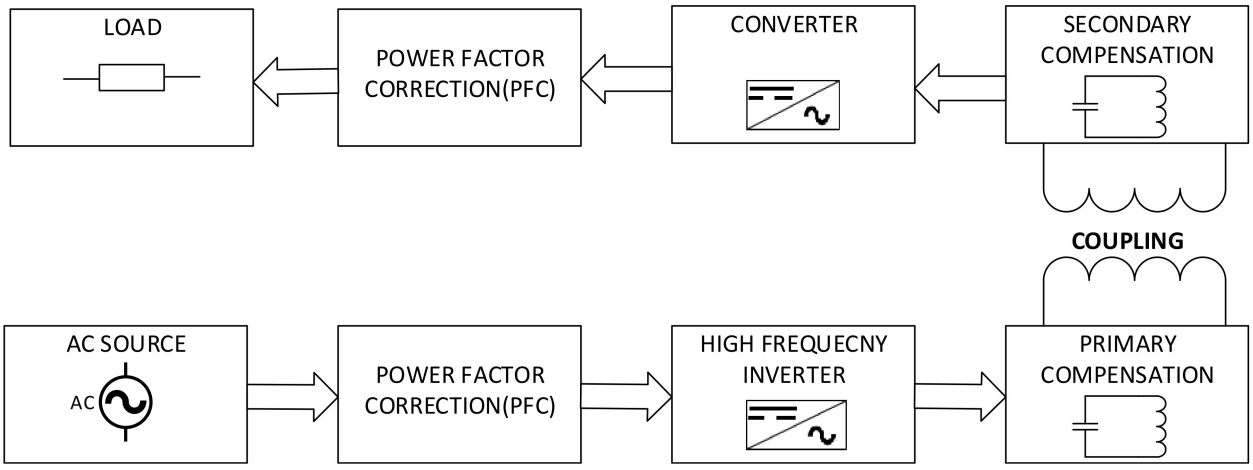

Figure 5. Block diagram of an IPT System.

In the system fed from an AC power supply, the output of the PFC is DC voltage and must be converted to AC voltage in order to create a time-varying magnetic field. A high frequency square wave is obtained by using a full bridge inverter. A current that starts flowing through the primary coil creates a time-varying magnetic field, which results with a voltage induced in the secondary coil. With the help of a full bridge rectifier, this voltage is rectified, and the current flows through the load that is connected to the output of the system.

4. Design Considerations in IPT Systems

In this part of the paper, critical design parameters of an IPT system are investigated in detail under subsections, and different system designs that have been studied in the literature are presented and discussed. First of all, a presentation of the critical design parameters that affect an efficient power transfer system is given in Figure 6.

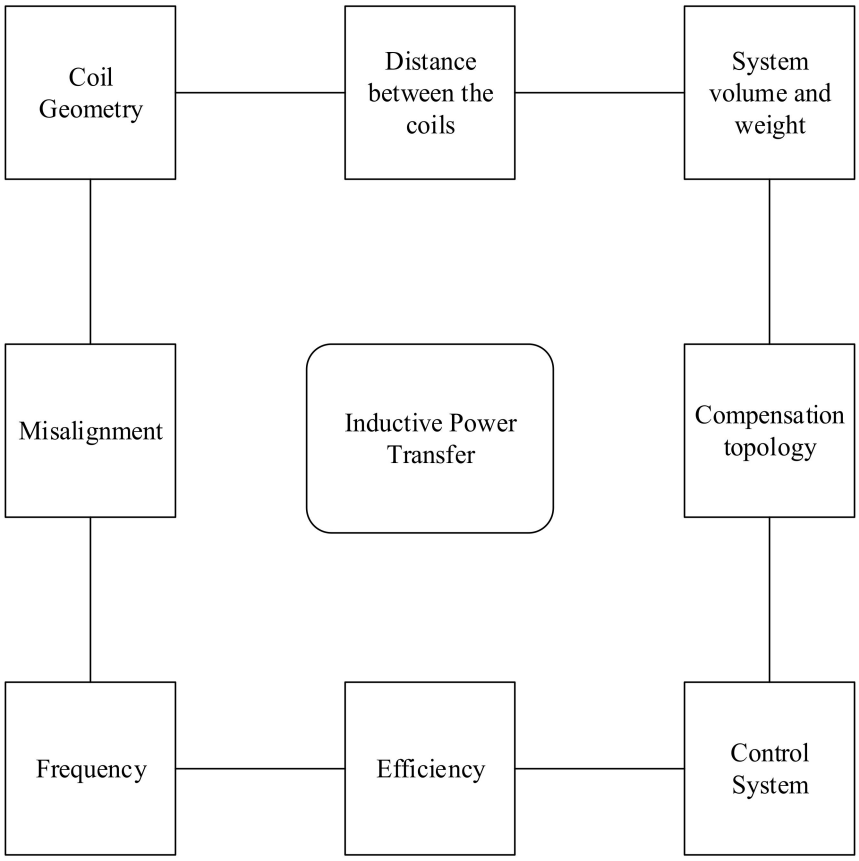

Figure 6. Overview of factors affecting an efficient IPT System.

4.1. Coil Design

Coil design is one of the most important and critical design parameters in IPT systems. It is possible to transfer desired power values with different coil shapes according to the application area and needs. While there are generally no restrictions on the size and shape of the primary coils, there are restrictions on the size of the secondary coils in particular. The main reason for this situation is that the secondary coil is located on the system to be charged, and it is desired to be as compact as possible. For example, since the secondary coils of electric vehicles are located under the vehicle chassis, the secondary coil can be in the dimensions reserved for this section at most. There are basic and widely used coil structures for IPT applications in the literature such as circular, rectangular, hexagonal and square. It is seen that mostly circular and rectangular-square structures are used in the literature [22,23]. The coupling coefficient, which is an important determinant of power transfer efficiency

and depends on the coil design, is desired to be as high as possible. In order to see the coupling coefficients of the basic coil structures, we performed the analysis of IPT coil models on ANSYS Maxwell 3-D electromagnetic finite element modelling software. With this analysis, the magnetic coupling performances of simple coil structures were examined, and these results are valuable in terms of giving behavioral insights to the designers. For a fair comparison, the coil area, conductor cross-section, the use of copper mass and the distance between the primary and secondary coils are the same for all structures, and $A_{area} = 4 \times 10^4$ mm^2, $A_w = 3.14$ mm^2, $m_{copper} = 7307$ mm^3 and $g = 50$ mm, respectively. The dimensions of different coil structures and coupling coefficient values are given in Table 1. Basic coil structures are given in Figure 7.

Table 1. Coil specifications and results.

Coil Shape	Parameter	Dimensions (mm)	Coupling Coefficient (*k*)
Circular	radius	112	0.269
Hexagonal	length of side	124	0.249
Rectangular	Length × width	141 × 282	0.209
Square	length of side	200	0.194

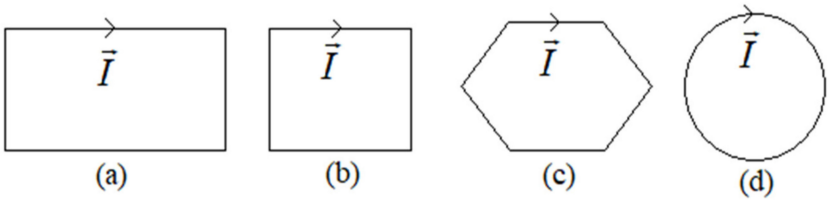

Figure 7. Coil shapes: (**a**) rectangular, (**b**) square, (**c**) hexagonal and (**d**) circular.

According to the results in Table 1, it is seen that the circular coil structure has the best coupling, and the hexagonal coil structure is the structure that gives the closest result to the circular. The coupling coefficients of the rectangular and square coil shapes are also very close to each other, and they are preferable structures.

For the transmission of a nominal power of 30 kW over a distance of 45 mm, 800 × 600 mm and identical rectangular coils with small ferrite cores on the edge of the coils were used on the primary and secondary sides [24]. The same research group also has another work with a coreless coil design [25]. A 2 kW power transfer was achieved with an 82% efficiency over a 150 mm distance by using a rectangular coil design [23]. A 3.7 kW application for EV charging system with rectangular coils was built and implemented [26]. In a study using a circular coil structure, the coil diameter was determined as 700 mm, and a parametric optimization method was used to ensure the use of minimum ferrite core. It was aimed to choose the most suitable design by placing 12 pieces of "I"-type ferrite cores in different sizes and shapes [27]. A 1 kW design with a flat spiral square coil design was proposed for mid-power EV charging [28]. Hexagonal coil was proposed to have a high coupling coefficient, more tolerance to misalignment and effective structure for multi-array coils such as honeycomb designs [29–32]. A circular coil structure is the most common, but it is particularly sensitive to misalignment. In addition, the length of the main flux path in the circular coil structure is one-fourth of the coil diameter, where this ratio is one-half for the novel coil structure called DD [33]. In another work, the dimensioning of the DD coil structure, which is one of the most commonly used, with widths from 300 mm to 1000 mm was investigated to provide WPT in large air gaps that can be used in charging the battery of all SUV- and sedan-type electric vehicles of different powers [34]. In an application where a DD structure is used, ferrite bars are placed at the end corners to prevent leakage fluxes, thereby reducing the leakage fluxes by 46% [35]. The article in which the BP (Bipolar Pad) design is proposed and compared with the DD structure is one of the important structures [36]. The BP pad is a new structure where the two windings are independent of each other and partially intersect. Their performance at 20 kHz frequency

was compared and 25% less copper was used, although it gave similar results with the DD structure. A ferrite-less DD structure with a reflection coil is proposed to design a cost-effective system [37].

Since the receiver coil is on the vehicle chassis, an important problem to be considered when designing the coil is the alignment problem that occurs between the primary and secondary coils. The effect of the variation in the distance between the primary and secondary coils and the misalignment on the coupling coefficient were investigated for a circular coil structure [38]. In order to investigate the effect of the misalignment on the system performance, the secondary coil shifted along the axis, and a high-efficiency power transmission region was obtained [39]. With ferrite bars, it is ensured that the flux stays between the primary and secondary coils, and a performance improvement is aimed for the alignment problem (zero region) with the DD coil structure and an additional Q coil, a structure called DDQ [33]. In a work aiming to solve the alignment problems with the suggestion of asymmetric coil structure, a maximum output power of 15 kW was obtained in the case of a 15 cm air gap and 400 mm lateral and 200 mm longitudinal misalignments. In addition, with the DOFA finite element method called Dominant Field Analysis, which provides convenience especially in the analysis of time-varying magnetic field vectors, the receiver and transmitter windings are designed independently of each other [40]. In recent years, new coil structures have been proposed specially to reduce the alignment tolerance and increase the coupling coefficient. One of these structures is called a QDQ (Quad D Quadrature) coil design. The outer large square coil has a 300 mm side length, and the diameter of the inner circular coil is 100 mm. The coils are electrically connected in parallel and magnetically in series. While the efficiency was 91.4% in perfect alignment, the efficiency decreased to 78% in the case of 50% lateral misalignment [41]. A cross shape of two rectangles coil structure was proposed to reduce the misalignment effect on the performance of the system. It has been shown that this design has less misalignment sensitivity and a higher coupling coefficient than circular and square coil shapes with low self-inductance values [42]. One of the most suggested structures in recent years to increase the coupling coefficient is the idea of adding auxiliary coils to the main coils, and they are called intermediate coils. The amount of flux produced and the coupling coefficient can be increased by adding one or more intermediate coils [43–45]. Thus, it is possible to increase the power transmission capacity and efficiency. The intermediate coils can be placed at any point between the primary and secondary coils with an independent compensation capacitor [46,47]. Since a flat spiral coil structure is used in electric vehicle applications, there are applications that are placed more in the area of the main coils [48–50]. A three-coil design with an assistive coil for the CC-CV charging of a battery was proposed in [51]. To increase the transfer distance, a multi-transmitter coil system is proposed in [52]. In [53], a new coil design named RC has been proposed and compared with DD design. An RC coil design requires less copper than a DD coil in terms of coupling performance.

As seen in Figure 8, mostly circular and rectangular coil structures are considered in literature. Apart from these basic structures, DD and intermediate coil structures have been emerging in recent years.

4.2. Operating Frequency, Power and Efficiency

One of the most important design parameters in WPT systems is the selection of the operating frequency, power and the targeted system efficiency. By choosing a high frequency value, while the coil sizes are reduced, especially the switching losses increase. In Figure 6, the operating frequencies encountered in the literature and the efficiency values obtained are shown. The operating frequency ranges used are concentrated in two bands. In most of the studies, a 20 kHz operating frequency was chosen. With the emergence of renewed interest in high frequency resonant WPT more than a decade ago, the objective was to stay out of the audible noise region within the constraints of the power electronics switches capabilities and their losses. With suitable switches, WPT systems having operating frequencies of hundreds of kilohertz have been reported. For automotive

EV charging, the WPT operating frequency was later standardized, and 85 kHz became the common resonant frequency for standardized charging power levels. This evolution can also be seen in Figure 9. Frequency selection determines the winding sizes and the number of turns to be used. As the frequency increases, the number of turns to be used in the primary and secondary decreases. However, constraints such as increased switching losses and semiconductor choices to be encountered in power electronics and interaction with other in-vehicle equipment should also be taken into account. In addition, high frequency values cause the current to flow from the surface, not through the conductor cross section, and this situation is defined as the skin effect. Especially in studies with high frequency values, the use of litz wire should be preferred. Thus, equal distribution of the current across the conductor cross-section is ensured and the skin effect can be reduced. Another parameter that the frequency value affects is the proximity effect. As the frequency value increases, the winding resistance increases, and the system efficiency decreases. With the use of Litz wire, the winding resistance decreases and losses are reduced.

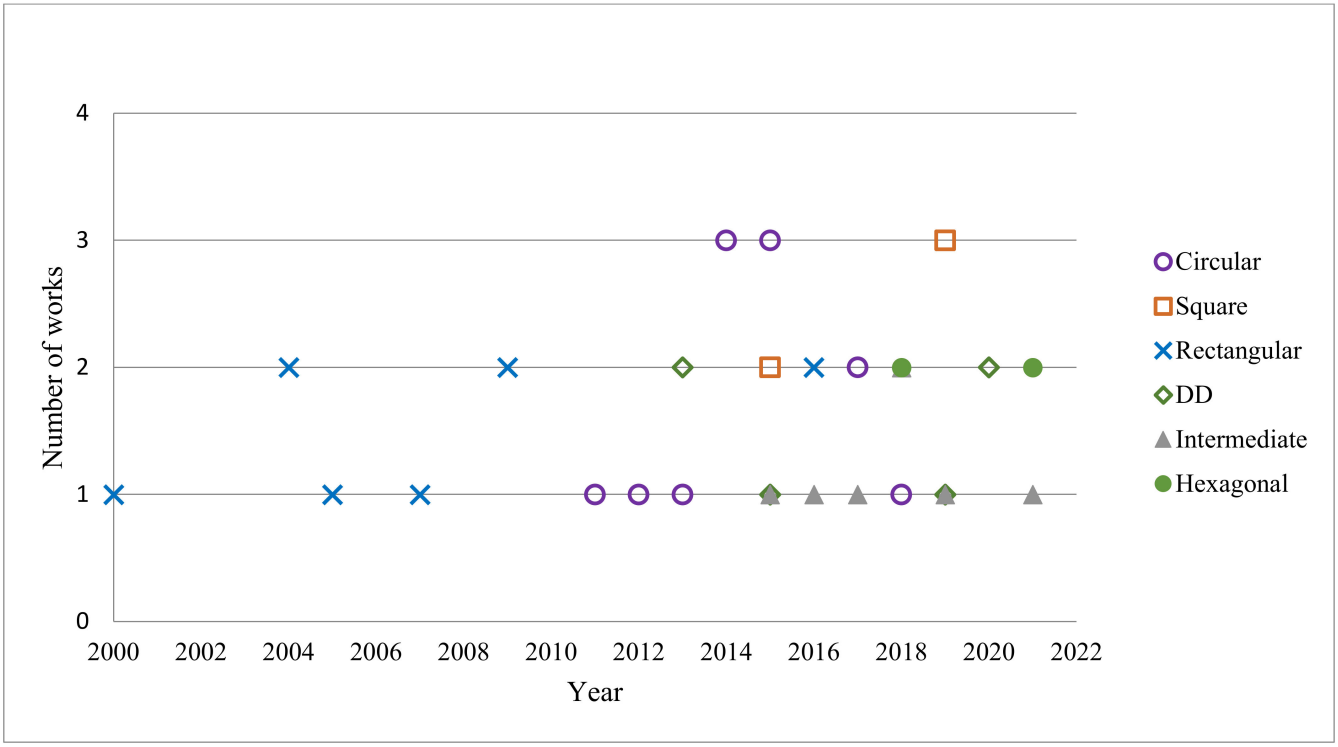

Figure 8. Number of works on coil structures used in academic studies by year of publication.

As seen from Figures 9 and 10, the frequency and efficiency values are increasing over the years. Efficiency values have been reaching more than 90–95% in recent years. In the first years, the operating frequency was chosen as 20 kHz in many applications. However, in recent years, parallel to the developments in semiconductor switching technologies, the value of the operating frequency has increased, and 85 kHz has gradually become a standard value for standard charging power levels. In addition, many commercial companies produce their products at two different frequencies, 20 kHz and 85 kHz. Figure 11 shows the variation of power values selected in academic studies on wireless charging of electric vehicle battery applications over the years. According to the graph, the most used power range is between 1 and 5 kW, and values of 3.3 and 3.7 kW are especially selected. There are some higher power values which are especially for EV buses. The power values of 3.7, 7, 11 and 22 kW have become standard charging values for EVs [54].

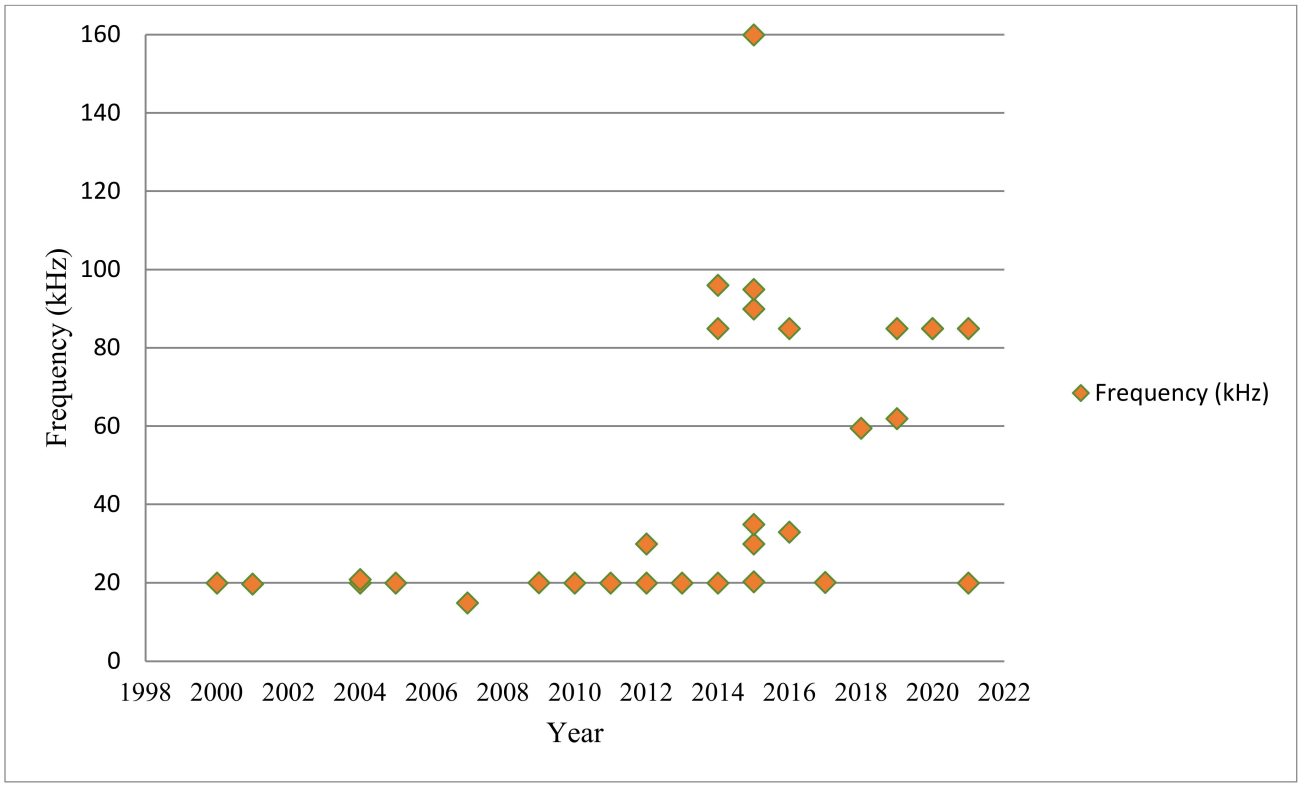

Figure 9. Frequency values used in academic studies by years of publication.

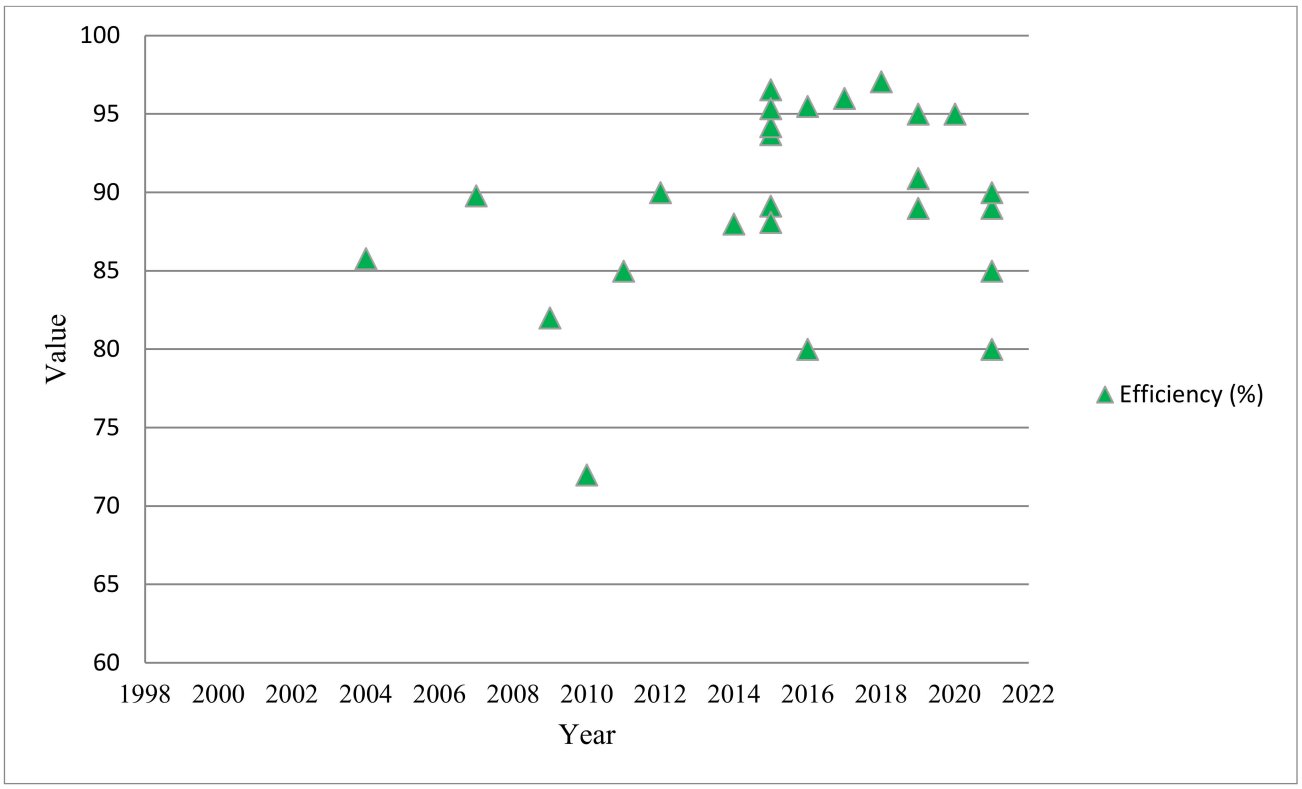

Figure 10. Efficiency values used in academic studies by years of publication.

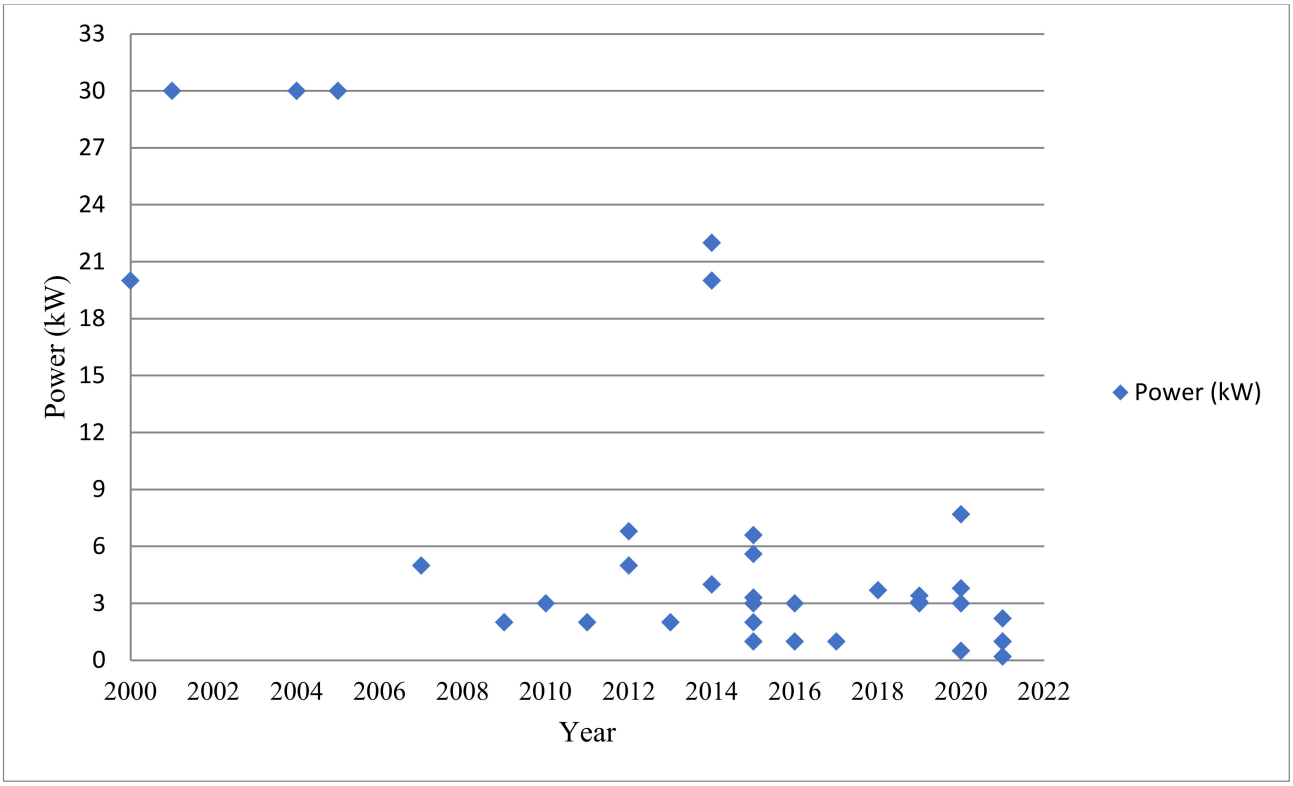

Figure 11. Power values selected in academic studies by years of publication.

4.3. Compensation Topology

The idea of transferring power over long distances and with higher efficiency gave rise to the idea of developing highly resonant systems. Despite the low coupling coefficient, the freedom of position for the secondary coil and the realization of high efficiency power transmission are important advantages [55]. In order to produce a sufficient magnetic field in WPT systems, it is aimed to reduce the total reactive power drawn by adding resonance capacitors suitable for the coil inductance values on the primary and/or secondary sides. Basically, while the purpose of the compensation on the primary side is to reduce the apparent power at the input, maximum power transfer is provided by eliminating the secondary inductance with the compensation capacitor added to the secondary side. At the same time, the output load value changes during battery charging. It becomes difficult to control the system, and in this case, control is facilitated with the help of compensation [56]. As a result, by adding compensation capacitors to the primary and secondary sides, the system can operate in resonance. The selection of the appropriate compensation topology depends on the requirements of the application, and there are quite different topologies. Compensation structures can be divided into two main groups, namely, four basic structures and hybrid topologies containing different combinations of these basic structures. The four basic structures can be listed as Series-Series (SS), Series-Parallel (SP), Parallel-Series (PS) and Parallel-Parallel (PP). These basic compensation structures are given in Figure 12.

In Table 2, the resonance capacitor equations for the basic topologies are given. The most important advantage of the SS topology is that the compensation capacitor values are independent of the resistive load and mutual inductance. It only depends on resonant frequency and self-inductance. Thanks to this advantage, the system remains in resonance and becomes less sensitive in case of misalignment. However, in the absence of the secondary coil, the primary coil will not be able to transfer its energy and will damage the primary side circuit. In case of misalignment, the mutual inductance value decreases, and hence, the coupling coefficient decreases. When the impedance equations seen by the source are examined (given in [23]), in the SS and SP topologies, the total impedance

decreases depending on the mutual inductance, while it causes the load on the secondary side, and therefore, the current drawn by the source at the input, to increase. In PS and PP topologies, while the total impedance increases, the current drawn from the source and the load decreases significantly. In PP and PS topologies, more complex equations are needed to calculate the primary capacitor, while the capacitor value depends on the mutual inductance and load values. Another disadvantage is that a current source is needed at the input in order to not be affected by instantaneous voltage changes [56]. In order to increase the efficiency of PP and PS structures and to provide an easier inverter current control, it is necessary to add extra inductance to the topology [57]. In [23], in a 200 kW design, the coil copper mass requirements for the same power value were compared for different compensation topologies. It was stated that the SS topology requires less copper and that the SP structure requires 4.6% more, PS requires 30% more and PP requires 24% more copper compared to the SS topology.

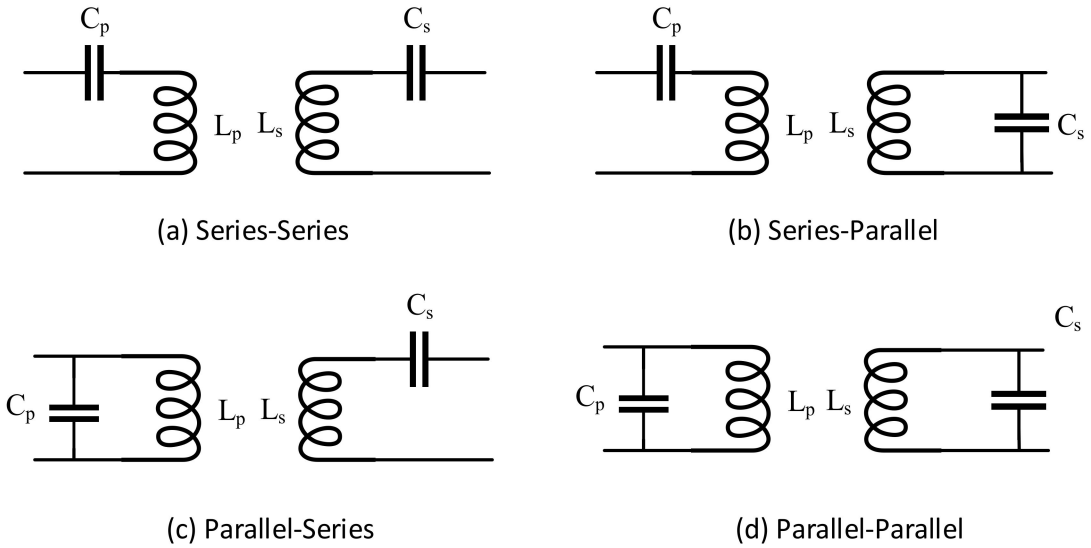

Figure 12. Basic compensation topologies.

Table 2. Compensation capacitor equations [25].

Topology	Primary Compensation Capacitor
SS	$C_p = \frac{1}{\omega_0^2 L_1}$
SP	$C_p = \frac{1}{\omega_0^2 \left(L_p - M^2/L_s\right)}$
PS	$C_p = \frac{L_p}{\left(\frac{\omega_0^2 M^2}{R_{load}}\right)^2 + \omega_0^2 {L_p}^2}$
PP	$C_p = \frac{L_p - M^2/L_s}{\left(\frac{M^2 R_{load}}{{L_s}^2}\right)^2 + \omega_0^2 \left(L_p - M^2/L_s\right)^2}$

In addition to the basic topologies, there are hybrid topologies proposed in the literature to bring the advantages of different topologies together. These hybrid topologies have advantages and disadvantages compared to each other [58]. For example, the CCL-S structure has an extra capacitor connected in series on the primary side, and thanks to this capacitor, it provides lower switching losses compared to the LC-S [59] structure. The output current and voltage values of the SS, S-LCL, S-CLC, and SP topologies are inversely proportional to the mutual inductance value, and the output power is inversely proportional to the square of the mutual inductance. In LCL-LCL, LCC-LCC, LCL-S, LCL-P, PS and PP topologies, the output current and voltage are directly proportional to the mutual

inductance while the output power increases proportionally to the square of the mutual inductance [60].

An application of hybrid compensation topology with CLC on the primary side LC on the secondary side was implemented [61]. When the application of LCC compensation for both sides is compared with an application of S/CLC, the S/CLC topology has less components with a higher power density [62]. A hybrid compensation topology was proposed for massive electric bicycles, and the performance was observed in the constant current-constant voltage operation mode [63].

In Figure 13 the number of works is given for the compensation topologies used in academic studies over the years. SS is the most selected topology for almost all application fields of WPT since it has great advantages. In recent years, the number of applications of hybrid compensation topologies are increasing. In Figure 13, the number of works for LCC and LCL are given separately from the hybrid topologies since they are the most selected topologies in hybrids.

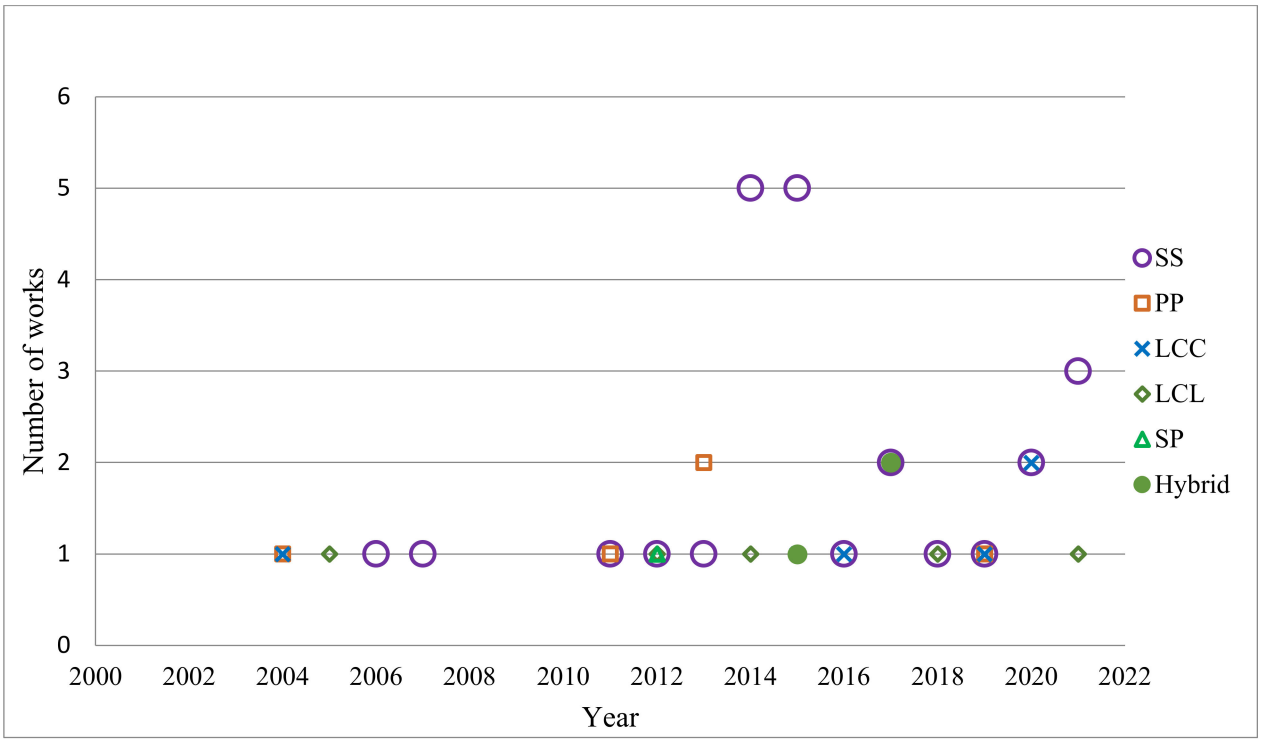

Figure 13. Number of works of compensation topologies used in academic studies by year of publication.

4.4. Health Issues

In the design of WPT systems, the effects of the targeted system on human health and its interaction with other devices should be considered. There are standards that various organizations have prepared and constantly update on this subject. The most important of these are listed as follows, and the frequency levels are given in Table 3:

- IEEE standard for determining the level of human exposure to radio frequency electromagnetic fields. Basic Specifications: 3 kHz to 300 GHz frequency range (2005–2019 versions available) [64];
- ICNIRP Guidelines for time-varying electric and magnetic field exposure limits. Basic Specifications: 1 Hz to 100 kHz frequency range, which means it is for low-frequency applications (LFA) [65];
- ICNIRP Guidelines for time-varying electric and magnetic field exposure limits. Basic Specifications: Frequency range, 100 kHz to 300 GHz, which means it is for high-frequency applications (HFA) [66]

- Canada Environmental and Radiation Health Sciences Directorate (ERHSD) guide for the protection of consumers from radiation. Basic Specifications: 3 kHz–300 GHz frequency range, 2015 [67];
- SAE (Society of Automotive Engineers) J2954 standard is a constantly updated standard for Electric vehicles and Plug-in Hybrid Electric vehicles in the power ranges from 3.7 kW to 22 kW, 2020 [54];
- The guidelines for Wireless Power systems prepared by the Broadband Wireless Forum Japan. It is a standard that can be used for applications operating in the frequency range of 10 kHz to 10 MHz, which was last updated in 2013 by a consortium formed by a group of researchers in 2009 [68].

Table 3. Frequency ranges for standards.

Health Standard	Frequency Range
IEEE	3 kHz–3 GHz
ICNIRP for LFA	1 Hz–100 kHz
ICNIRP for HFA	100 kHz–300 GHz
ERHSD	3 kHz–300 GHz
SAE	80 kHz–90 kHz.
Wireless forum of JAPAN	10 kHz–10 MHz

The most used and frequently updated guidelines on EMC issues on WPT systems are listed in [69]. The most widely used of these standards are IEEE, ICNIRP and SAE, and updated versions of these standards can be purchased for a fee. The variation in and comparison of exposure values allowed by ICNIRP and IEEE standards over the years are given in [70]. The threshold values for electric and magnetic field density allowed according to the ICNIRP standard are relatively lower than other standards. While creating the standards, the frequency values are roughly divided into low and high frequencies. While 1 Hz–100 kHz is considered as a low-frequency region, values of 100 kHz–300 GHz and above are considered as high-frequency regions and are published according to this separation in the standards. One hundred kilohertz is considered as a limit value, and when working above this value, the effect of heating effects should be taken into account, and the Specific Absorption Rate (SAR) value should be calculated. Studies have shown that if the human body is exposed to frequency values from 10 MHz to several GHz, the body temperature will increase by 1 to 2 °C. In addition, there are studies showing that there is an increase in childhood leukemia and various types of cancer in cases of long-term exposure. However, it is not possible to make a definite judgment about the small number of subjects in the studies and whether exposure was the root of the problems.

The conductivity (S/m) and relative permittivity (F/m) values for relevant human tissues at 100 kHz frequency are given in [71]. In order not to exceed the permissible threshold values, many methods have been proposed in the literature and supported by studies. A shielding sensor coil was proposed for reducing the leakage magnetic field for a 500 W WPT system, and the measurement results were compared to SAE standards [72]. Magnetic field density values for a 2 kW WPT system with an operating frequency of 20 kHz, which is the frequency range commonly used in electric vehicle applications, are investigated and measured in terms of human exposure can be shown as an example study [27]. An aluminum plate is used as shielding to reduce magnetic field density values in this work. In order to show the effect of aluminum shielding effect on magnetic field density values of a 1 kW WPT system with an operating frequency of 20 kHz and hexagonal coil, the 3D model was created and analyzed on ANSYS Maxwell [30]. The FEA (Finite Element Analyses) results show that the aluminum shielding has a significant effect on reducing the magnetic field density. The results are given in Figure 14.

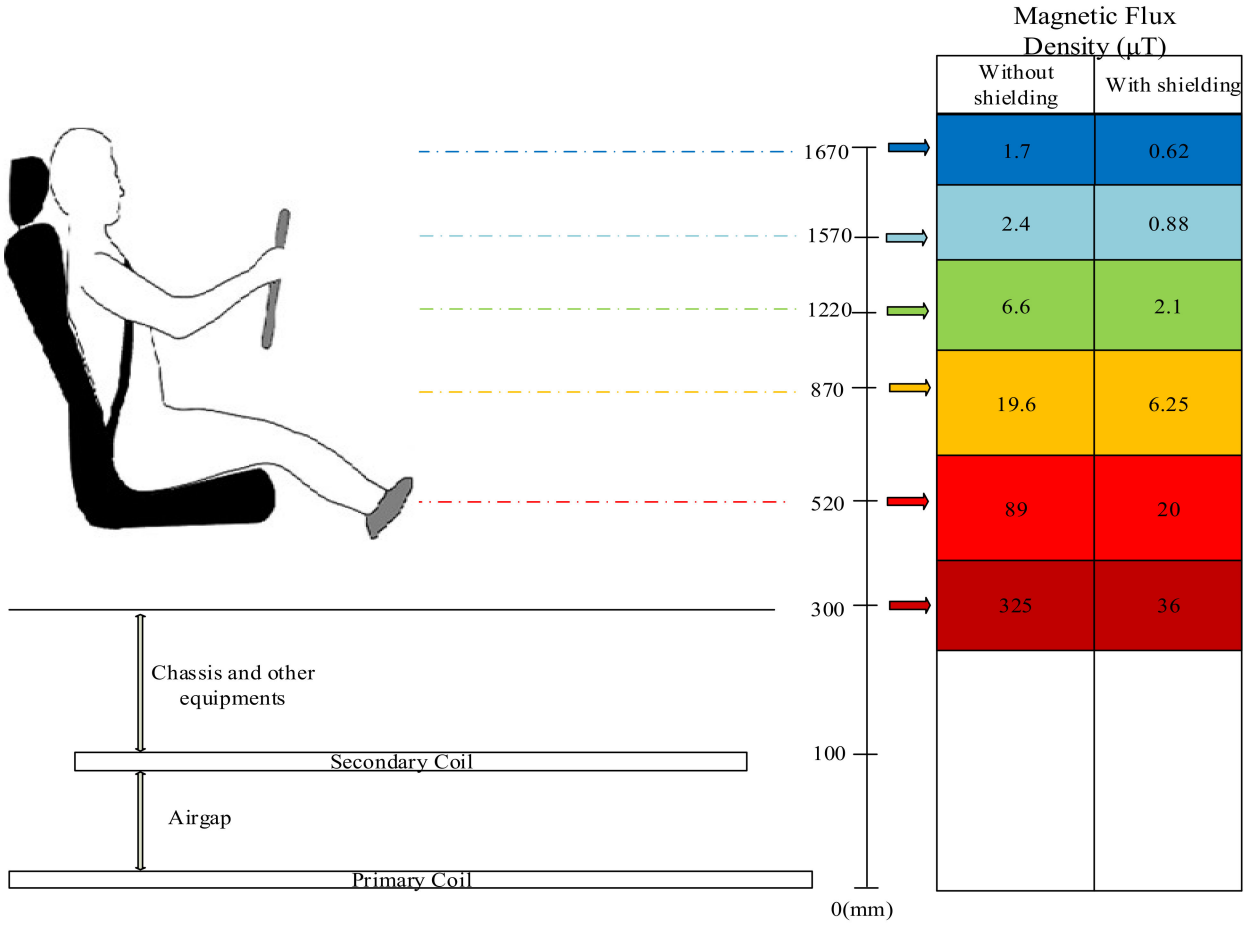

Figure 14. Effect of aluminum shielding on magnetic field density values [30].

In a study conducted at the University of Wisconsin, Madison, it was aimed to have low electric field and magnetic field density values in the air gap at powers at the kW level. With a six-step design, the optimal system parameters were obtained, and a design in accordance with health standards was obtained [70]. Since it is operated at high frequencies (a few MHz), losses increase due to proximity and skin effects. In order to reduce these losses, the performances of different types of conductor cross-sections were studied, and a new conductor cross-section shape was proposed [73]. Although the use of aluminum as shielding provides significant success, it causes an increase in eddy losses. In order to eliminate this, by adding auxiliary coils, the magnetic flux remains between the primary and secondary coils, and a design in accordance with health standards is proposed [74].

4.5. Control System

The best switching frequency, the most suitable passive components and switches can be selected according to defined objectives and desired trade-offs using the optimization algorithms. The switching frequency is based on the losses and applied control techniques. These control techniques are explained in this section.

4.5.1. Controller Location

The control techniques of wireless power transfer (WPT) typically aim to regulate battery the CC/CV charging. A comparison of CC and CC/CV charging for a WPT system is well studied in [75]. The results show that CC charging has a little higher efficiency than the CC/CV method, and the CV stage takes most of the charging time. Generally, these control techniques consist of three parts which are primary-side control, secondary-side control and dual-sided control [76]. Wireless communication transmits the SoC data from

the secondary side to the primary side as illustrated in Figure 15 [77]. To design a series-series compensated primary controlled IPT battery charging system, the controller location is very important because of the required and sufficient data to be obtained [78].

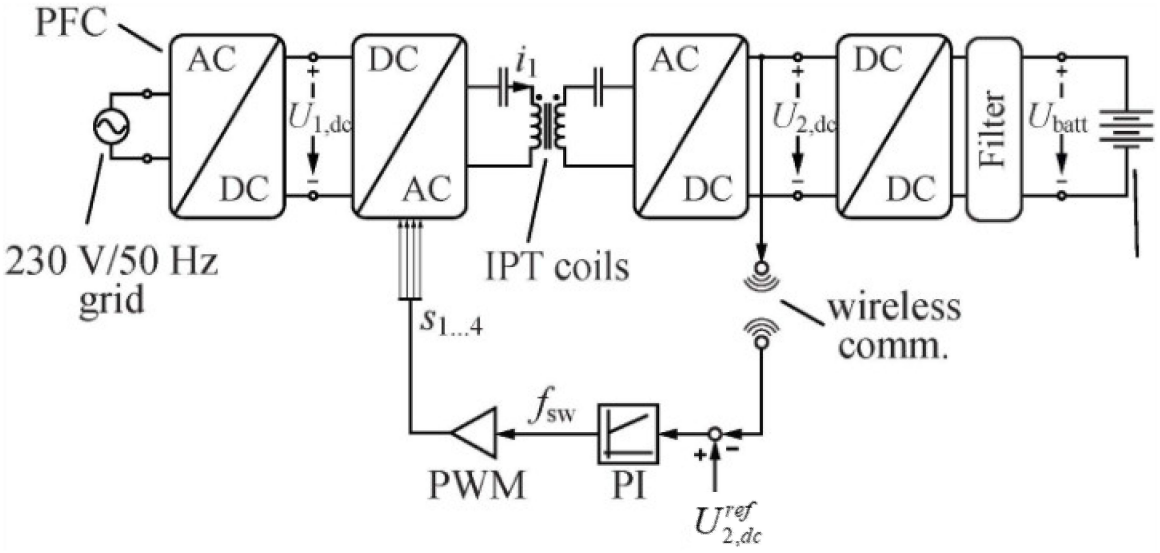

Figure 15. Block diagram of a series-series compensated primary controlled IPT battery charging system [78].

The active rectification is required by the secondary-side control. In addition, this control is used in the multiple pick-up coils connected applications [79–84]. However, both full bridge and active rectifiers are controlled to manage the power flow to the load by the dual-sided control [81–84]. To achieve maximum efficiency for multiple receivers by determining an optimum primary side current and load resistance, a closed-form equation was proposed [85]. For a three-coil system, the load-independent output current system was investigated, and the results show that there are two different operating frequency to achieve constant output current [86]. Implementation of a uniform voltage gain control system for misalignment conditions is given and studied [87]. Three-phase charging based on an equivalent three-phase grid connected inverter is given in Figure 16.

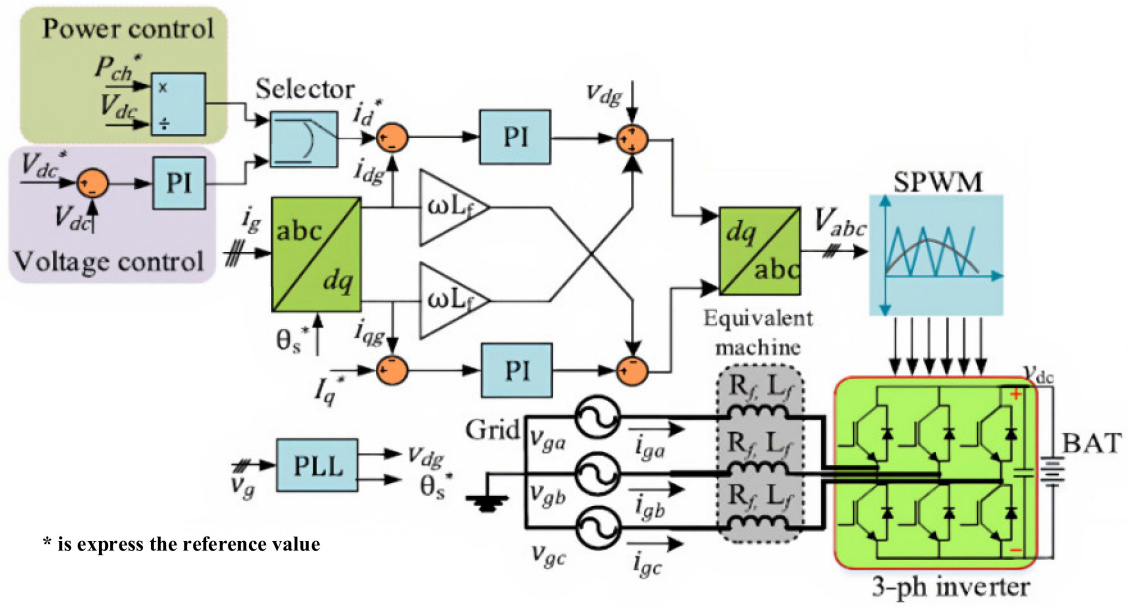

Figure 16. Three phase charging based on equivalent three-phase grid connected inverter [82].

4.5.2. Control Variable

A control law of a WPT should keep track of:

- Output (battery) voltage, battery current and SOC;
- Reactive power and WPT network impedance;
- Maximum efficiency.

A variation in either the phase shift between the two converter bridge legs, the switching frequency or the DC-link voltage occurs [76,77,88]. The basic voltage equations can be written with fundamental frequency and depicted AC equivalent circuit in Figure 17 for IPT, where M is the mutual inductance of the transformer:

$$v_1 = -j\omega M \times i_2 \tag{3}$$

$$v_2 = j\omega M \times i_1 \tag{4}$$

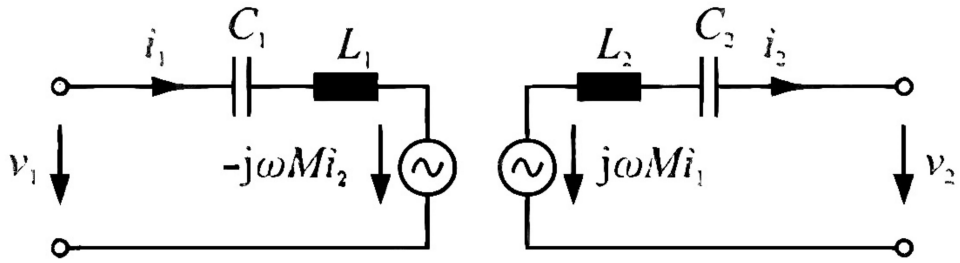

Figure 17. Equivalent circuit for fundamental frequency approximation of IPT [88].

As it can be seen from these equations, although the load current reduces, transmitter current is related to output voltage, and therefore, it remains the same for constant output voltage applications, i.e., battery charging. Resulting in a reduced efficiency due to the conduction losses of the switches and the resonant circuit for light load conditions [89]. This problem can be solved by implementing a half-controlled or fully controlled rectifier and employing a dual-side phase shift control as explained in [90].

In order to control the output power, the switching frequency is increased to operate in the region, where resonant tank impedance Zin is higher and the primary current i1, as well as the transmitted power, is reduced. In case of magnetic coupling or load variations occur, it may take time to settle to new operating point with frequency modulation, and excessive output voltage may be observed during this transition [88]. Another important drawback of this control method is high conduction losses, especially at light load conditions caused by the increased reactive power as a consequence of the frequency detuning [89,90]. Dual (self-sustained) control of IPT is giving in Figure 18 [90].

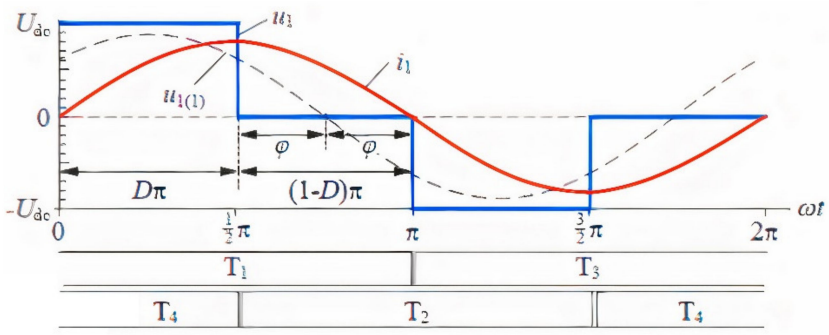

Figure 18. Dual (self-sustained) Control of IPT [90].

In [89], it is reported that a desired load performance can be achieved with the constant switching frequency operation at the resonant frequency of the IPT and the two DC-link

voltages U1 and U2 are used to control the output power. Control methods regarding bi-directional power transfer are elaborated in [90]. The IPT-based control strategies to transfer wireless power on the H-bridge inverter are phase shift control and frequency control.

5. Discussion

This paper has reviewed the development history and fundamentals of the Inductive Power Transfer technology with a comprehensive review of the design of coil structures, compensation topologies, health issues, control systems, selection of the operating frequency and power ranges for EV applications. A comparison of basic coil structures in terms of coupling coefficient has been performed by using ANSYS and Maxwell 3D FEM software. According to analysis results, the circular coil structure has the best coupling coefficient, and it is the most widely studied coil structure in the literature. The DD and intermediate coil structures are receiving attention in recent years. In the first years of the technology, a 20 kHz operating frequency was a typical choice. However, with the development of semiconductor technology higher frequencies have been used and 85 kHz became a standard for electric vehicle charging at standardized power levels up to 22 kW. The primary and secondary sides need to be compensated in a high-efficient IPT system with compensation capacitors. Series-Series (SS) compensation is the most used topology, especially for EV battery charging applications. IPT systems have an effect on human health, and this effect should be considered during the design. There are several standards published and constantly updated on this issue. Applied control techniques have been discussed. These discussions and reviews show that IPT systems will have a significant role in the charging of EVs in the next years. From a technical view some of the literature gaps and ideas for future works are as follows:

(a) High-power transfer with smaller size coils and smaller compensation topologies, which will make the system lighter and lower cost;
(b) The role of the WPT systems in fast and extreme fast charging technologies since the charging time is still a problem for EVs;
(c) The effect of time-varying electric and magnetic field in WPT systems on consumer health need further detail studies and EMC problems should be discussed;
(d) Grid management according to Static and Dynamic WPT systems and Vehicle-to-Grid (V2G) technology through Wireless EV charging;
(e) Modular systems for WPT applications are receiving more attention these days and the power range of this type of applications could be varies from low power to high power;
(f) Electrifying roads are another hot topic for this technology, which is under development in some pilot projects around the world and expect to be commercially available in the near future.

According to the state-of-the-art, higher switching frequencies, novel coil designs and various compensation topologies will be proposed in the next future.

Author Contributions: E.A. wrote and reviewed the first version of the paper; A.A. contributed to writing the control section, reviewing and editing the paper; M.E.B. reviewed and improved the editing of the paper; M.T.A. and O.H. reviewed and edited the manuscript and supervised this research study. All authors have read and agreed to the published version of the manuscript.

Funding: This research received no external funding.

Data Availability Statement: Not applicable.

Acknowledgments: MOBI acknowledges Flanders Make for their support to the research group.

Conflicts of Interest: The authors declare no conflict of interest.

Appendix A

Table A1. Most cited articles in the literature.

Work	Year	Frequency (kHz)	Airgap (mm)	Power (kW)	Core	Coil Structure	C.Topology	Efficiency (%)
[91]	2000	20	N/A	20	N/A	N/A	N/A	N/A
[24]	2001	19.7	45	30	Yes	Rectangular	N/A	N/A
[92]	2004	20	45	30	No	Rectangular	PP	N/A
[93]	2004	20.9	45	30	No	Rectangular	LCL-P	85.8
[25]	2005	20	45	30	No	Rectangular	LCL-P	N/A
[1]	2007	14.9	200	5	No	Rectangular	SS	89.8
[23]	2009	20.1	150	2	No	Rectangular	SS	82
[94]	2010	20	170	3	N/A	N/A	N/A	72
[27]	2011	20	100	2	Yes	Circular	PP	85
[95]	2012	20	255	5	Yes	Circular	LCL	90
[96]	2012	30	N/A	6.8	N/A	N/A	SS	N/A
[33]	2013	20	200	2	Yes	DD, DDQ	PP	N/A
[97]	2014	165	150	4	No	Circular	SS	N/A
[98]	2014	96	40	4	Yes	Circular	SS	N/A
[99]	2014	20	N/A	20	N/A	N/A	LCL	88
[100]	2014	85	N/A	22	N/A	N/A	SS	N/A
[101]	2015	160	203.2	1	No	Square	SS	93.7
[102]	2015	30	150	2	Yes	Circular	SS	89.15
[103]	2015	35	135	3	Yes	Circular	SS	94.2
[104]	2015	90	200	3.3	No	Intermediate	SS	96.56
[105]	2015	95	150	5.6	Yes	DD	LCC	95.36
[106]	2015	20.3	120	6.6	No	Circular	SS	88.1
[107]	2015	N/A	100	N/A	No	Circular	SS	90
[41]	2016	33	300	1	No	Intermediate	SS	80
[108]	2017	85	150	3	Yes	Rectangular	LCC	95.5
[109]	2017	20.15	185	1	Yes	Circular	SS	96
[50]	2018	59.5	200	3.7	No	Intermediate	SS	97.08
[110]	2019	62	300	3	Yes	Square	SS	90.9
[37]	2019	85	175	3.4	Yes	DD	PP	89
[111]	2019	85	150	3.09	Yes	Intermediate	LCC	95
[112]	2020	85	150	7.7	No	Rectangular	SS	N/A
[113]	2020	85	200	3	Yes	BP	Hybrid	95
[114]	2020	85	N/A	3.8	N/A	Circular	LCL	N/A
[115]	2020	85	N/A	0.5	Yes	Circular	LCC	95
[116]	2021	85	175	2.2	Yes	Intermediate	SS	89
[117]	2021	85	150	1	No	Intermediate	LCL	90
[30]	2021	20	100	1	No	Hexagonal	SS	85
[32]	2021	85	100	0.2	No	Hexagonal	SS	80

References

1. Villa, J.L.; Lombart, A.; Sanz, J.F.; Sallan, J. Practical Development of a 5 kW ICPT System SS Compensated with a Large Air gap. In Proceedings of the 2007 IEEE International Symposium on Industrial Electronics, Vigo, Spain, 4–7 June 2007; pp. 1219–1223.
2. Jang, Y.; Jovanovic, M.M. A contactless electrical energy transmission system for portable-telephone battery chargers. *IEEE Trans. Ind. Electron.* **2003**, *50*, 520–527. [CrossRef]
3. Ram Rakhyani, A.K.; Mirabbasi, S.; Chiao, M. Design and Optimization of Resonance-Based Efficient Wireless Power Delivery Systems for Biomedical Implants. *IEEE Trans. Biomed. Circuits Syst.* **2011**, *5*, 48–63. [CrossRef]
4. Ma, H.; Yang, Y.; Qi, N.; Ma, S.; Li, X. Demonstration of a high-efficiency MWPT System for Aerospace. In Proceedings of the 2018 IEEE Wireless Power Transfer Conference (WPTC), Montreal, QC, Canada, 3–7 June 2018; pp. 1–4.
5. Zhu, D.; Grabham, N.J.; Clare, L.; Stark, B.H.; Beeby, S.P. Inductive power transfer in e-textile applications: Reducing the effects of coil misalignment. In Proceedings of the 2015 IEEE Wireless Power Transfer Conference (WPTC), Boulder, CO, USA, 13–15 May 2015; pp. 1–4.
6. Sealy, K.D.; Efe, V.; Patterson, S.M.; Bohm, R.J.; Kesler, M.P. Wireless Power Transfer for a Seat-Vest-Helmet System. U.S. Patent US20150115733A1, 30 April 2015.
7. Mohamed, A.A.S.; Lashway, C.R.; Mohammed, O. Modeling and Feasibility Analysis of Quasi-Dynamic WPT System for EV Applications. *IEEE Trans. Transp. Electrif.* **2017**, *3*, 343–353. [CrossRef]
8. Jang, Y.J.; Jeong, S.; Lee, M.S. Initial Energy Logistics Cost Analysis for Stationary, Quasi-Dynamic, and Dynamic Wireless Charging Public Transportation Systems. *Energies* **2016**, *9*, 483. [CrossRef]
9. Hertz, H.; Mulligan, J.F. *Heinrich Rudolf Hertz (1857–1894): A Collection of Articles and Addresses*; Garland Pub: New York, NY, USA, 1994.

10. Massie, W.W.; Underhill, C.R. The future of the wireless art. In *Wireless Telegraphy and Telephony*; D. Van Nostrand: New York, NY, USA, 1908; pp. 67–71.
11. Hutin, M.; Leblanc, M. Transformer System for Electric Railways. U.S. Patent 527,857, 23 October 1894.
12. Brown, W.C. The history of wireless power transmission. *Solar Energy* **1996**, *56*, 3–21. [CrossRef]
13. Abel, E.; Third, S. Contactless power transfer—An exercise in topology. *IEEE Trans. Magn.* **1984**, *20*, 1813–1815. [CrossRef]
14. Delmas, A.; Omeich, M.; Rioux, C. High efficiency inductive energy transfer. In Proceedings of the 7th Pulsed Power Conference, Monterey, CA, USA, 11–14 June 1989; pp. 598–601.
15. Esser, A. Contactless charging and communication for electric vehicles. *IEEE Ind. Appl. Mag.* **1995**, *1*, 4–11. [CrossRef]
16. Eghtesadi, M. Inductive power transfer to an electric vehicle-analytical model. In Proceedings of the 40th IEEE Conference on Vehicular Technology, Orlando, FL, USA, 6–9 May 1990; pp. 100–104.
17. Elliott, G.A.J.; Boys, J.T.; Green, A.W. Magnetically coupled systems for power transfer to electric vehicles. In Proceedings of the 1995 International Conference on Power Electronics and Drive Systems (PEDS 95), Singapore, 21–23 February 1995; Volume 2, pp. 797–801.
18. Kurs, A.; Karalis, A.; Moffatt, R.; Joannopoulos, J.D.; Fisher, P.; Soljacic, M. Wireless Power Transfer via Strongly Coupled Magnetic Resonances. *Science* **2007**, *317*, 83–86. [CrossRef]
19. Kline, M.; Izyumin, I.; Boser, B.; Sanders, S. Capacitive power transfer for contactless charging. In Proceedings of the 2011 Twenty-Sixth Annual IEEE Applied Power Electronics Conference and Exposition (APEC), Fort Worth, TX, USA, 6–11 March 2011; pp. 1398–1404. [CrossRef]
20. Dai, J.; Ludois, D.C. A Survey of Wireless Power Transfer and a Critical Comparison of Inductive and Capacitive Coupling for Small Gap Applications. *IEEE Trans. Power Electron.* **2015**, *30*, 6017–6029. [CrossRef]
21. Yang, Y.; Cui, J.; Cui, X. Design and Analysis of Magnetic Coils for Optimizing the Coupling Coefficient in an Electric Vehicle Wireless Power Transfer System. *Energies* **2020**, *13*, 4143. [CrossRef]
22. Bosshard, R.; Mühlethaler, J.; Kolar, J.W.; Stevanović, I. Optimized magnetic design for inductive power transfer coils. In Proceedings of the 28th Applied Power Electronics Conference and Exposition (APEC), Long Beach, CA, USA, 17–21 March 2013; pp. 1812–1819.
23. Sallan, J.; Villa, J.L.; Llombart, A.; ve Sanz, J.F. Optimal design of ICPT systems applied to electric vehicle battery charge. *IEEE Trans. Ind. Electron.* **2009**, *56*, 2140–2149. [CrossRef]
24. Wang, C.-S.; Covic, G.A.; Stielau, O.H. General stability criterions for zero phase angle controlled loosely coupled inductive power transfer systems. In Proceedings of the IECON'01. 27th Annual Conference of the IEEE Industrial Electronics Society (Cat. No.37243), Denver, CO, USA, 29 November–2 December 2001; Volume 2, pp. 1049–1054.
25. Wang, C.S.; Stielau, O.H.; Covic, G.A. Design considerations for a contactless electric vehicle battery charger. *IEEE Trans. Ind. Electron.* **2005**, *52*, 1308–1314. [CrossRef]
26. Yang, Y.; El Baghdadi, M.; Lan, Y.; Benomar, Y.; Van Mierlo, J.; Hegazy, O. Design Methodology, Modeling, and Comparative Study of Wireless Power Transfer Systems for Electric Vehicles. *Energies* **2018**, *11*, 17176. [CrossRef]
27. Budhia, M.; Covic, G.A.; Boys, J.T. Design and Optimization of Circular Magnetic Structures for Lumped Inductive Power Transfer Systems. *IEEE Trans. Power Electron.* **2011**, *26*, 3096–3108. [CrossRef]
28. Kosesoy, Y.; Aydin, E.; Yildiriz, E.; Aydemir, M.T. Design and Implementation of a 1-kW Wireless Power Transfer System for EV Charging. In Proceedings of the IEEE 13th International Conference on Compatibility, Power Electronics and Power Engineering (CPE-POWERENG), Sonderborg, Denmark, 23–25 April 2019.
29. Aydin, E.; Kosesoy, Y.; Yildiriz, E.; Aydemir, M.T. Comparison of Hexagonal and Square Coils for Use in Wireless Charging of Electric Vehicle Battery. In Proceedings of the IEEE 2018 International Symposium on Electronics and Telecommunications (ISETC), Timisoara, Romania, 8–9 November 2018.
30. Aydin, E.; Aydemir, M.T. A 1-kw wireless power transfer system for electric vehicle charging with hexagonal flat spiral coil. *Turk. J. Electr. Eng. Comput. Sci.* **2021**, *29*, 2346–2361. [CrossRef]
31. Tan, P.; Yi, F.; Liu, C.; Guo, Y. Modeling of Mutual Inductance for Hexagonal Coils with Horizontal Misalignment in Wireless Power Transfer. In Proceedings of the IEEE Energy Conversion Congress and Exposition (ECCE), Portland, OR, USA, 23–27 September 2018.
32. Tan, P.; Peng, T.; Gao, X.; Zhang, B. Flexible Combination and Switching Control for Robust Wireless Power Transfer System with Hexagonal Array Coil. *IEEE Trans. Power Electron.* **2021**, *36*, 3868–3882. [CrossRef]
33. Budhia, M.; Boys, J.T.; Covic, G.A.; Huang, C.-Y. Development of a Single-Sided Flux Magnetic Coupler for Electric Vehicle IPT Charging Systems, Industrial Electronics. *IEEE Trans.* **2013**, *60*, 318–328.
34. Nagendra, G.R.; Covic, G.A.; Boys, J.T. Determining the Physical Size of Inductive Couplers for IPT EV Systems. *IEEE J. Emerg. Sel. Top. Power Electron.* **2014**, *2*, 571–583. [CrossRef]
35. Lin, F.Y.; Zaheer, A.; Budhia, M.; Covic, G.A. Reducing leakage flux in IPT systems by modifying pad ferrite structures. In Proceedings of the IEEE Energy Conversion Congress and Exposition (ECCE), Pittsburgh, PA, USA, 14–18 September 2014; pp. 1770–1777.
36. Zaheer, A.; Kacprzak, D.; Covic, G.A. A bipolar receiver pad in a lumped IPT system for electric vehicle charging applications. In Proceedings of the IEEE Energy Conversion Congress and Exposition (ECCE), Raleigh, NC, USA, 15–20 September 2012; pp. 283–290.

37. Pearce, M.G.S.; Covic, G.A.; Boys, J.T. Robust Ferrite-Less Double D Topology for Roadway IPT Applications. *IEEE Trans. Power Electron.* **2019**, *34*, 6062–6075. [CrossRef]
38. Zheng, C.; Ma, H.; Lai, J.S.; Zhang, L. Design Considerations to Reduce Gap Yesiation and Misalignment Effects for the Inductive Power Transfer System. *IEEE Trans. Power Electron.* **2015**, *30*, 6108–6119. [CrossRef]
39. Dang, Z.; Qahouq, J.A.A. Modeling and investigation of magnetic resonance coupled wireless power transfer system with lateral misalignment. In Proceedings of the 2014 IEEE Applied Power Electronics Conference and Exposition—APEC, Fort Worth, TX, USA, 16–20 March 2014.
40. Choi, S.Y.; Huh, J.; Lee, W.Y.; Rim, C.T. Asymmetric Coil Sets for Wireless Stationary EV Chargers with Large Lateral Tolerance by Dominant Field Analysis. *IEEE Trans. Power Electron.* **2014**, *29*, 6406–6420. [CrossRef]
41. Kalwar, K.A.; Mekhilef, S.; Seyedmahmoudian, M.; Horan, B. Coil Design for High Misalignment Tolerant Inductive Power Transfer System for EV Charging. *Energies* **2016**, *9*, 937. [CrossRef]
42. Sis, S.A.; Orta, E. A Cross-Shape Coil Structure for Use in Wireless Power Applications. *Energies* **2018**, *11*, 1094. [CrossRef]
43. Ahn, D.; Hong, S. A Study on Magnetic Field Repeater in Wireless Power Transfer. *IEEE Trans. Ind. Electron.* **2013**, *60*, 360–371. [CrossRef]
44. Kim, J.; Son, H.; Kim, K.; Park, Y. Efficiency Analysis of Magnetic Resonance Wireless Power Transfer with Intermediate Resonant Coil. *IEEE Antennas Wirel. Propag. Lett.* **2011**, *10*, 389–392. [CrossRef]
45. Lee, C.K.; Zhong, W.X.; Hui, S.Y.R. Effects of Magnetic Coupling of Nonadjacent Resonators on Wireless Power Domino-Resonator Systems. *IEEE Trans. Power Electron.* **2012**, *27*, 1905–1916. [CrossRef]
46. Hatchavanich, N.; Sangswang, A.; Konghirun, M. Effects of Intermediate Coil Position in a Triple-Coil Series-Series Compensation in Wireless Power Transfer. In Proceedings of the IEEE International Symposium on Circuits and Systems (ISCAS), Sapporo, Japan, 26–29 May 2019; pp. 1–5.
47. Hatchavanich, N.; Sangswang, A.; Konghirun, M. Operational Region of Novel Multi-Coil Series-Series Compensation in Wireless Power Transfer System for Electric Vehicle Applications. In Proceedings of the IEEE International Symposium on Circuits and Systems (ISCAS), Sapporo, Japan, 26–29 May 2019; pp. 1–5.
48. Moon, S.; Kim, B.; Cho, S.; Ahn, C.; Moon, G. Analysis and Design of a Wireless Power Transfer System with an Intermediate Coil for High Efficiency. *IEEE Trans. Ind. Electron.* **2014**, *61*, 5861–5870. [CrossRef]
49. Marques, E.G.; Marques, C.; Silva, J.V.N.; da Silva, S.V.; Perdigão, M.S.; Mendes, A.M.S. Evaluation of intermediate coils in IPT systems under magnetic coupler displacements. In Proceedings of the IECON 2017—43rd Annual Conference of the IEEE Industrial Electronics Society, Beijing, China, 29 October–1 November 2017; pp. 5342–5347. [CrossRef]
50. Tran, D.H.; Vu, V.B.; Choi, W. Design of a High-Efficiency Wireless Power Transfer System with Intermediate Coils for the On-Board Chargers of Electric Vehicles. *IEEE Trans. Power Electron.* **2018**, *33*, 175–187. [CrossRef]
51. Xu, H.; Huang, Z.; Yang, Y.; Huang, Z.; Iam, I.-W.; Lam, C.-S. Analysis and Design of Three-Coil Coupler for Inductive Power Transfer System with Automatic Seamless CC-to-CV Charging Capability. *IEEE Access* **2022**, *10*, 10139–10148. [CrossRef]
52. Jeon, S.J.; Seo, D.-W. Effect of Additional Transmitting Coils on Transfer Distance in Multiple-Transmitter Wireless Power Transfer System. *IEEE Access* **2022**, *10*, 9174–9183. [CrossRef]
53. Mohammed, M.H.; Ameen, Y.M.Y.; Mohamed, A.A.S. A Combined Rectangular/Circular Power Pad for Electric Vehicles Wireless Charging. In Proceedings of the 2021 IEEE Green Technologies Conference (GreenTech), Virtual, 7–9 April 2021; pp. 195–200.
54. SAE (Society of Automotive Engineers). *J2954 Standard is a Constantly Updated Standard for Electric Vehicles and Plug-In Hybrid Electric Vehicles in the Power Ranges from 3.7 kW to 22 kW*; SAE: Atlanta, GA, USA, 2020.
55. Morris, K. *Highly Resonant Wireless Power Transfer: Safe, Efficient, and over Distance*; Witricity Co.: Watertown, MA, USA, 2017.
56. Zhang, W.; Mi, C.C. Compensation Topologies of High-Power Wireless Power Transfer Systems. *IEEE Trans. Veh. Technol.* **2016**, *65*, 4768–4778. [CrossRef]
57. Moradewicz, A.J.; Kazmierkowski, M.P. Contactless Energy Transfer System With FPGA-Controlled Resonant Converter. *IEEE Trans. Ind. Electron.* **2010**, *57*, 3181–3190. [CrossRef]
58. Shevchenko, V.; Husev, O.; Strzelecki, R.; Pakhaliuk, B.; Poliakov, N.; Strzelecka, N. Compensation Topologies in IPT Systems: Standards, Requirements, Classification, Analysis, Comparison and Application. *IEEE Access* **2019**, *7*, 120559–120580. [CrossRef]
59. Wang, Y.; Yao, Y.; Liu, X.; Xu, D.; Cai, L. An LC/S Compensation Topology and Coil Design Technique for Wireless Power Transfer. *IEEE Trans. Power Electron.* **2018**, *33*, 2007–2025. [CrossRef]
60. Houran, A.M.; Yang, X.; Chen, W. Magnetically Coupled Resonance WPT: Review of Compensation Topologies, Resonator Structures with Misalignment, and EMI Diagnostics. *Electronics* **2018**, *11*, 22. [CrossRef]
61. Samanta, S.; Rathore, A.K. A New Current-Fed CLC Transmitter and LC Receiver Topology for Inductive Wireless Power Transfer Application: Analysis, Design, and Experimental Results. *IEEE Trans. Transp. Electrif.* **2015**, *1*, 357–368. [CrossRef]
62. Wang, Y.; Yao, Y.; Liu, X.; Xu, D. S/CLC Compensation Topology Analysis and Circular Coil Design for Wireless Power Transfer. *IEEE Trans. Transp. Electrif.* **2017**, *3*, 496–507. [CrossRef]
63. Chen, Y.; Kou, Z.; Zhang, Y.; He, Z.; Mai, R.; Cao, G. Hybrid Topology With Configurable Charge Current and Charge Voltage Output-Based WPT Charger for Massive Electric Bicycles. *IEEE J. Emerg. Select. Top. Power Electron.* **2018**, *6*, 1581–1594. [CrossRef]
64. *IEEE Std C95*; IEEE Standard for Safety Levels with Respect to Human Exposure to Radio Frequency Electromagnetic Fields, 3 kHz to 300 GHz Amendment. IEEE: New York, NY, USA, 2005; pp. 1–9.

65. ICNIRP. Guidelines for limiting exposure to time-Yesying electric and magnetic fields (1 Hz–100 kHz). *Health Phys.* **2010**, *99*, 818–836. [CrossRef]
66. International Commission on Non-Ionizing Radiation Protection. ICNIRP statement on the Guidelines for limiting exposure to time-Yesying electric, magnetic, and electromagnetic fields (up to 300 GHz). *Health Phys.* **2009**, *97*, 257–258. [CrossRef]
67. Canada Environmental and Radiation Health Sciences Directorate (ERHSD). *Guide for the Protection of Consumers from Radiation, Basic Specifications: 3 KHZ—300 GHz*; Canada Environmental and Radiation Health Sciences Directorate: Ottawa, ON, Canada, 2015.
68. Broadband Wireless Forum. *Guidelines for the Use of Wireless Power Transmission Technologies, Version 1.0*; Broadband Wireless Forum: London, UK, 2007.
69. Obayashi, S.; Tsukahara, H. EMC issues on wireless power transfer. In Proceedings of the 2014 International Symposium on Electromagnetic Compatibility, Tokyo, Japan, 4–8 August 2014; pp. 601–604.
70. Zhu, G.; Lorenz, R.D. Achieving low magnetic flux density and low electric field intensity for an inductive wireless power transfer system. In Proceedings of the IEEE Energy Conversion Congress and Exposition (ECCE), Cincinnati, OH, USA, 16–18 February 2017.
71. Mohamed, C.; Guillaume, V.; Alexandru, T. Compliance Assessment of Human Body Exposure to Wireless Power Systems. In Proceedings of the 2nd World Congress on Electrical Engineering and Computer Systems and Science (EECSS'16), Orleans, ON, Canada, 16–17 August 2016.
72. Son, S.; Woo, S.; Kim, H.; Ahn, J.; Huh, S.; Lee, S.; Ahn, S. Shielding Sensor Coil to Reduce the Leakage Magnetic Field and Detect the Receiver Position in Wireless Power Transfer System for Electric Vehicle. *Energies* **2022**, *15*, 2493. [CrossRef]
73. Lee, S.; Lorenz, R.D. Development and validation of model for 95% efficiency, 220 W wireless power transfer over a 30 cm air-gap. In Proceedings of the IEEE Energy Conversion Congress and Exposition, Atlanta, GA, USA, 12–16 September 2010.
74. Chiang, C. Wireless charging system with magnetic field shaping for electric vehicles. In Proceedings of the the World Electric Vehicle Symposium and Exhibition (EVS27), Barcelona, Spain, 17–20 November 2013; pp. 1–5.
75. Wang, Z.; Wei, X. Design Considerations for Wireless Charging Systems with an Analysis of Batteries. *Energies* **2015**, *8*, 10664–10683. [CrossRef]
76. Bosshard, R.; Badstubner, U.; Kolar, J.W.; Stevanovic, I. Comparative evaluation of control methods for inductive power transfer. In Proceedings of the 2012 International Conference on Renewable Energy Research and Applications (ICRERA), Nagasaki, Japan, 11–14 November 2012; pp. 1–6.
77. Bosshard, R.; Kolar, J.W.; Wunsch, B. Control method for inductivepower transfer with high partial-load efficiency and resonance tracking. In Proceedings of the 2014 International Power Electronics Conference (IPEC-Hiroshima 2014-ECCE ASIA), Hiroshima, Japan, 18–21 May 2014; pp. 2167–2174.
78. Nguyen, B.X.; Vilathgamuwa, D.M.; Foo, G.H.B.; Wang, P.; Ong, A.; Madawala, U.K.; Nguyen, T.D. An efficiency optimization schemefor bidirectional inductive power transfer systems. *IEEE Trans. Power Electron.* **2014**, *30*, 6310–6319. [CrossRef]
79. Colak, K.; Asa, E.; Bojarski, L.M.; Czarkowski, D.; Onar, O.C. A novelphase-shift control of semibridgeless active rectifier for wireless powertransfer. *IEEE Trans. Power Electron.* **2015**, *30*, 6288–6297. [CrossRef]
80. Li, K.; Zhao, H.; Liu, Q.; Shi, Y.; Wang, C.; Zhang, P.; Wang, L. Design of novel coil structure for wireless power transfer system supporting multi-load and 2-D free-positioning. *Electr. Eng.* **2021**, *103*, 2009–2020. [CrossRef]
81. Yeo, T.-D.; Kwon, D.; Khang, S.-T.; Yu, Y.-W. Design of maxi-mum efficiency tracking control scheme for closed-loop wireless powercharging system employing series resonant tank. *IEEE Trans. Power Electron.* **2016**, *32*, 471–478. [CrossRef]
82. Patil, D.; Mcdonough, M.K.; Miller, J.M.; Fahimi, B.; Balsara, P.T. Wireless power transfer for vehicular applications: Overviewand challenges. *IEEE Trans. Transp. Electrif.* **2017**, *4*, 3–37. [CrossRef]
83. Dai, X.; Li, X.; Li, Y.; Hu, A.P. Maximum efficiency trackingfor wireless power transfer systems with dynamic coupling coefficientestimation. *IEEE Trans. Power Electron.* **2017**, *33*, 5005–5015. [CrossRef]
84. Li, Y.; Hu, J.; Chen, F.; Li, Z.; He, Z.; Mai, R. Dual-phase-shift controlscheme with current-stress and efficiency optimization for wirelesspower transfer systems. *IEEE Trans. Circuits Syst. Regul. Pap.* **2018**, *65*, 3110–3121. [CrossRef]
85. Lee, W.; Lee, W.; Ahn, D. Maximum Efficiency Conditions Satisfying Power Regulation Constraints in Multiple-Receivers Wireless Power Transfer. *Energies* **2022**, *15*, 3840. [CrossRef]
86. Sun, L.; Tang, H.; Zhang, Y. Determining the Frequency for Load-Independent Output Current in Three-Coil Wireless Power Transfer System. *Energies* **2015**, *8*, 9719–9730. [CrossRef]
87. Gao, Y.; Farley, K.B.; Tse, Z.T.H. A Uniform Voltage Gain Control for Alignment Robustness in Wireless EV Charging. *Energies* **2015**, *8*, 8355–8370. [CrossRef]
88. Mai, R.; Liu, Y.; Li, Y.; Yue, P.; Cao, G.; He, Z. An Active-Rectifier-Based Maximum Efficiency Tracking Method Using an Additional Measurement Coil for Wireless Power Transfer. *IEEE Trans. Power Electron.* **2018**, *33*, 716–728. [CrossRef]
89. Feng, H.; Tavakoli, R.; Onar, O.C.; Pantic, Z. Advances in High-Power Wireless Charging Systems: Overview and Design Considera-tions. *IEEE Trans. Transp. Electrif.* **2020**, *6*, 886–919. [CrossRef]
90. Metwly, M.Y.; Abdel-Majeed, M.S.; Abdel-Khalik, A.S.; Hamdy, R.A.; Hamad, M.S.; Ahmed, S. A Review of Integrated On-Board EV Battery Chargers: Advanced Topologies, Recent Developments and Optimal Selection of FSCW Slot/Pole Combination. *IEEE Access* **2020**, *8*, 85216–85242. [CrossRef]

91. Wang, C.-S.; Stielau, O.H.; Covic, G.A. Load models and their application in the design of loosely coupled inductive power transfer systems. In Proceedings of the PowerCon 2000, International Conference on Power System Technology, (Cat. No. 00EX409), Perth, WA, Australia, 4–8 December 2000; Volume 2, pp. 1053–1058.
92. Wang, C.-S.; Covic, G.A.; Stielau, O.H. Power transfer capability and bifurcation phenomena of loosely coupled inductive power transfer systems. *IEEE Trans. Ind. Electron.* **2004**, *51*, 148–157. [CrossRef]
93. Wang, C.-S.; Covic, G.A.; Stielau, O.H. Investigating an LCL load resonant inverter for inductive power transfer applications. *IEEE Trans. Power Electron.* **2004**, *19*, 995–1002. [CrossRef]
94. Lee, S.; Huh, J.; Park, C.; Choi, N.; Cho, G.; Rim, C. On-Line Electric Vehicle using inductive power transfer system. In Proceedings of the 2010 IEEE Energy Conversion Congress and Exposition, Atlanta, GA, USA, 12–16 September 2010; pp. 1598–1601.
95. Wu, H.H.; Gilchrist, A.; Sealy, K.D.; Bronson, D. A High Efficiency 5 kW Inductive Charger for EVs Using Dual Side Control. *IEEE Trans. Ind. Inform.* **2012**, *8*, 585–595. [CrossRef]
96. Bac, N.X.; Vilathgamuwa, D.M.; Madawala, U.K. A matrix converter based Inductive Power Transfer system. In Proceedings of the 2012 10th International Power & Energy Conference (IPEC), Ho Chi Minh City, Vietnam, 12–14 December 2012; pp. 509–514.
97. Huang, Z.; Wong, C.; Tse, C.K. Design methodology of a series-series inductive power transfer system for electric vehicle battery charger application. In Proceedings of the 2014 IEEE Energy Conversion Congress and Exposition (ECCE), Pitsburgh, PA, USA, 14–18 September 2014; pp. 1778–1782.
98. Chen, R.; Zheng, C.; Zahid, Z.U.; Faraci, E.; Yu, W.; Lai, J.S.; Senesky, M.; Anderson, D.; Lisi, G. Analysis and parameters optimization of a contactless IPT system for EV charger. In Proceedings of the 2014 IEEE Applied Power Electronics Conference and Exposition—APEC, Fort Worth, TX, USA, 16–20 March 2014; pp. 1654–1661.
99. Rahnamaee, H.R.; Madawala, U.K.; Thrimawithana, D.J. A multi-level converter for high power-high frequency IPT systems. In Proceedings of the 2014 IEEE 5th International Symposium on Power Electronics for Distributed Generation Systems (PEDG), Galway, Ireland, 24–27 June 2014; pp. 1–6.
100. Schumann, P.; Blum, O.; Eckhardt, J.; Henkel, A. High efficient, compact vehicle power electronics for 22kW inductive charging. In Proceedings of the 2014 4th International Electric Drives Production Conference (EDPC), Nuremberg, Germany, 30 September–1 October 2014; pp. 1–5.
101. Asa, E.; Colak, K.; Bojarski, M.; Czarkowski, D. A novel multi-level phase-controlled resonant inverter with common mode capacitor for wireless EV chargers. In Proceedings of the 2015 IEEE Transportation Electrification Conference and Expo (ITEC), Dearborn, MI, USA, 14–17 June 2015; pp. 1–6.
102. Ibrahim, M.; Pichon, L.; Bernard, L.; Razek, A.; Houivet, J.; Cayol, O. Advanced Modeling of a 2-kW Series–Series Resonating Inductive Charger for Real Electric Vehicle. *IEEE Trans. Veh. Technol.* **2015**, *64*, 421–430. [CrossRef]
103. Diekhans, T.; De Doncker, R.W. A Dual-Side Controlled Inductive Power Transfer System Optimized for Large Coupling Factor Variations and Partial Load. *IEEE Trans. Power Electron.* **2015**, *30*, 6320–6328. [CrossRef]
104. Moon, S.; Moon, G.W. Wireless Power Transfer System with an Asymmetric Four-Coil Resonator for Electric Vehicle Battery Chargers. *IEEE Trans. Power Electron.* **2015**, *31*, 6844–6854.
105. Deng, J.; Li, W.; Nguyen, T.D.; Li, S.; Mi, C.C. Compact and Efficient Bipolar Coupler for Wireless Power Chargers: Design and Analysis. *IEEE Trans. Power Electron.* **2015**, *30*, 6130–6140. [CrossRef]
106. Lee, J.Y.; Han, B.M. A Bidirectional Wireless Power Transfer EV Charger Using Self-Resonant PWM. *IEEE Trans. Power Electron.* **2015**, *30*, 1784–1787. [CrossRef]
107. Agcal, A.; Bekiroglu, N.; Ozcira, S. Examination of Efficiency Based on Air Gap and Characteristic Impedance Variations for Magnetic Resonance Coupling Wireless Energy Transfer. *J. Magn.* **2015**, *20*, 57–61. [CrossRef]
108. Kan, T.; Nguyen, T.D.; Wjite, J.C.; Malhan, R.K.; Mi, C.C. A New Integration Method for an Electric Vehicle Wireless Charging System Using LCC Compensation Topology. *IEEE Trans. Power Electron.* **2017**, *3*, 1638–1650. [CrossRef]
109. Kim, H.; Song, C.; Kim, D.; Jung, D.H.; Kim, I.; Kim, Y.; Kim, J.; Ahn, S.; Kim, J. Coil Design and Measurements of Automotive Magnetic Resonant Wireless Charging System for High-Efficiency and Low Magnetic Field Leakage. *IEEE Trans. Microw. Theory Tech.* **2017**, *64*, 383–400. [CrossRef]
110. Lu, W.; Dong, Y.; Shen, J.; Chen, X. Implementation of High-Power & Low-Frequency Resonant Wireless Power Transfer Charging System for Electric Vehicles. In Proceedings of the IEEE 10th International Symposium on Power Electronics for Distributed Generation Systems (PEDG), Xi'an, China, 3–6 June 2019.
111. Kan, T.; Lu, F.; Nguyen, T.; Mercier, P.P.; Mi, C.C. Integrated Coil Design for EV Wireless Charging Systems Using LCC Compensation Topology. *IEEE Trans. Power Electron.* **2018**, *33*, 9231–9241. [CrossRef]
112. Grazian, F.; Shi, W.; Soeiro, T.B.; Dong, J.; van Duijsen, P.; Bauer, P. Compensation Network for a 7.7 kW Wireless Charging System that Uses Standardized Coils. In Proceedings of the 2020 IEEE International Symposium on Circuits and Systems (ISCAS), Seville, Spain, 12–14 October 2020; pp. 1–5.
113. Zhou, J.; Yao, P.; Guo, K.; Cao, P.; Zhang, Y.; Ma, H. A Heterogeneous Inductive Power Transfer System for Electric Vehicles with Spontaneous Constant Current and Constant Voltage Output Features. *Electronics* **2020**, *9*, 1978. [CrossRef]
114. Ruddell, S.; Madawala, U.K.; Thrimawithana, D.J. A Wireless EV Charging Topology With Integrated Energy Storage. *IEEE Trans. Power Electron.* **2020**, *35*, 8965–8972. [CrossRef]
115. Ramezani, A.; Narimani, M. Optimized Electric Vehicle Wireless Chargers with Reduced Output Voltage Sensitivity to Misalignment. *IEEE J. Emerg. Sel. Top. Power Electron.* **2020**, *8*, 3569–3581. [CrossRef]

116. Marques, E.G.; Mendes, A.M.S.; Perdigão, M.S.; Costa, V.S. Design Methodology of a Three Coil IPT System with Parameters Identification for EVs. *IEEE Trans. Veh. Technol.* **2021**, *70*, 7509–7521. [CrossRef]
117. Zhang, P.; Saeedifard, M.; Onar, O.C.; Yang, Q.; Cai, C. A Field Enhancement Integration Design Featuring Misalignment Tolerance for Wireless EV Charging Using LCL Topology. *IEEE Trans. Power Electron.* **2021**, *36*, 3852–3867. [CrossRef]